REMOVAL OF ARSENATE AND ARSENITE BY CALCINED NANOCRYSTALINE LAYERED DOUBLE HYDROXIDES

by

Eman Rashad Mihoub Wahbah

A thesis submitted to the faculty of
The University of Utah
in partial fulfillment of the requirements for the degree of

Master of Science

Department of Metallurgical Engineering

The University of Utah

August 2015

The University of Utah Graduate School

STATEMENT OF THESIS APPROVAL

The thesis of **Eman Rashad Mihoub Wahbah**

has been approved by the following supervisory committee members:

Manoranjan Misra	, Chair	**12/05/2014**
		Date Approved
Raj K. Rajamani	, Member	**12/05/2014**
		Date Approved
Swomitra Mohanty	, Member	**12/05/2014**
		Date Approved

and by **Manoranjan Misra** , Chair of

the Department of **Metallurgical Engineering**

and by David B. Kieda, Dean of The Graduate School.

ABSTRACT

This work studies the removal of arsenic (V), arsenate, and arsenic (III), arsenite, from aqueous solution using calcined Quintinite-3T (Al/Mg mixed oxides) and calcined La-LDHs (La/Mg mixed oxides). The two adsorbents Quintinite-3T and La-LDHs were prepared, calcined at different temperatures, and characterized by XRD, BET, and SEM. The surface area of the calcined Quintinite-3T was 193.4 m^2/g, while the surface area of the calcined La-LDHs was 112.4 m^2/g. The particles size ranged from 12 to 56 nm for the uncalcined Quintinite-3T and from 24

to 42 nm for the calcined Quintinite-3T. The particle size ranged from 27 to 56 nm for as-synthesized La-LDHs and from 18 to 35 nm for the calcined La-LDHs. Also, new hybrid adsorbent was synthesized and characterized as well. Kinetic analysis, adsorption isotherm, and factors affecting the adsorption were investigated. Calcined Quintinite-3T retained As(v) and did not release it back to water even after an entire month.

The adsorption of As(V) and As(III) by calcined La-LDHs increased with time up to 2 weeks and 1 month, respectively.

TABLE OF CONTENTS

LIST OF TABLES

ACKNOWLEDGMENTS

I would like to express my gratitude to all those who had supported me and helped me a lot to do this work. First, I must acknowledge and thank Allah, my God, for uncountable blessings and for protecting and guiding me in this work, and I have to avow that without of Allah's help I couldn't do anything.

I would like to express my gratitude to my supervisor, Professor Manoranjan Misra, whose expertise and understanding added considerably to my graduate experience. I appreciate his vast knowledge and skill in many areas. Many thanks go to Dr. Monalisa Panda for training and guiding me through my work. I would like to thank Professor Swomitra Mohanty for his expert advice and instructions. I would like to thank supervisory committee member, Professor Raj K. Rajamani, for the time and effort to review my work.

I am grateful to my parents, parents-in-law, my brother, and my sisters for the support they provided me through my entire life. Special appreciation to my parents, who helped me a lot by their kindly emotions and their prayers for me. I dedicate this work to my parents.

Sincere appreciation and thanks go to my beloved husband and best friend, Mohassab, without whose love, encouragement, and assistance I would not have finished this thesis.

Special thanks go to the light of my life, my daughter, Noor. I have to say that she

spent much time far off me to finish this work. She has been fond of SEM micrographs of nanomaterials. At her age of 4, Noor is considering pursuing a master's degree in "nano graphene"—in her words!

CHAPTER 1

REMOVAL OF ARSENATE AND ARSENITE BY NANOCRYSTALINE CALCINED QUINTINITE-3T

1.1. Introduction

Arsenic occurs in the drinking water of many countries all over the world, such as Bangladesh, West Bengal, Argentina, Vietnam, China, Mexico, Nepal, India, Hungary, Australia, USA, and Canada, in the form of As(III), arsenite, and As(V), arsenate [1–4]. As(III) is more difficult to be removed than As(V), but fortunately As(III) exists mostly in anaerobic ground water [5]. The occurrence of arsenic in the ground water is mainly due to minerals dissolved naturally from weathered rocks and soils over time or by human activities [6]. Arsenic is very harmful for humans, animals, and plants. Long-term exposure to As can cause hyperkeratosis, skin lesions, and various types of cancers [7], including skin and bladder cancers [8]. The Environmental Protection Agency (EPA) of the US limited arsenic concentration in drinking water to 50 ppb, and they changed this limit later to 5 ppb [8]. Many researchers have studied arsenic removal by various adsorbents, such as steel making slag [1], mesoporous alumina [9], zirconium-manganese binary hydrous oxide [10], rutile ore [11], layered double hydroxides (LDHs) [7, 12], and some nanofibers as titanate nanofibers [13], titania nanofibers [14], and polyvinyl alcohol/Fe^{3+} nanofibers [5].

Quintinite-3T (Q-3T) is a natural mineral, a family member of LDHs, with a chemical formula of $Mg_4Al_2(OH)_{12}CO_3•4(H_2O)$ [15]. Its synthesis is economically viable and an easily scalable process [4]. With calcination, Q-3T is converted to Al/Mg mixed oxides. Calcined LDHs (at about temperature 500 ˚C) are better than uncalcined LDHs in the adsorption of oxyanions [12]. This is due to the fact that by calcining LDHs at 450 to 500 ˚C, LDHs lose their original layer structure and form highly active composite metal oxides with high thermal stability, large surface area, and high stability against sintering even under extreme conditions [16]. In addition calcination in this temperature range increases the surface area due to the additional mesoporous regions such as channels and pores formed from the removal of water and carbon dioxide [12]. Moreover, the competing ions have a stronger effect on arsenic adsorption on the uncalcined LDHs than on the calcined LDHs [12].

In this study calcined Quintinite-3T adsorbent was investigated for the removal of As(V) and As(III) from water. Q-3T was calcined at different temperatures: 200 ˚C, 300 ˚C, 400 ˚C, and 500 ˚C. The effect of aging on calcined Q-3T was explored from 30 min to 1 month. The adsorbent was characterized before and after adsorption. In addition, new adsorbent (calcined mixture of Q-3T and diatomaceous powder) was tested for arsenic removal. All adsorbents were characterized by SEM, XRD, and BET. Arsenic was quantitatively determined by ICP-MS.

1.2. Experimental Details

1.2.1. Materials

All chemicals were used without further purification. Arsenate solution was prepared from $Na_2HAsO_4.7H_2O$ (98%) and deionized water (18.2 MΩcm). Arsenite solution was prepared from As_2O_3 (99.996%) and deionized water.

1.2.2. Adsorbent Preparation

The Al/Mg solution was prepared by dissolving 56.98 g of $Mg(NO_3)_2.6H_2O$ and 41.68 g of $Al(NO_3)_3.9H_2O$ in 100 mL of deionized water. The NaOH solution was prepared by dissolving 20.00 g of NaOH to 13.626 g of Na_2CO_3 in 100 mL of deionized water. Then 45 mL of Mg/Al solution were added to 70 mL of NaOH solution under stirring at 400 rpm and temperature of 60 ˚C for 24 hours in an oil bath. The precipitate was washed by deionized water, dried at 120 ˚C, and then calcined at 500 ˚C.

1.2.3. Characterization of the Absorbent

To identify the different phases in the synthesized adsorbent (before and after calcination; and after adsorption), the fine powder was introduced into a Rigaku MiniFlex 600 X-ray diffractometer supplied by Rigaku (The Woodlands, TX) and equipped with K_β foil filter Cu K_α radiation (λ = 1.5406 Å). The X-ray intensity was measured over 2θ (θ: diffraction angel) from 10 to 100° with a scanning rate of 0.02 °/s. To determine the morphology and particle size of the adsorbent, a Hitachi S-4800 SEM supplied by Hitachi (Tokyo, Japan) was used. The SEM was equipped with an X-MAX tool for EDS analysis. The accelerating voltage was selected to be 10+ kV to enable the quantitative analysis of

all the elements of interest.

In order to determine the average surface area of the adsorbent, volumetric N_2 sorption studies were undertaken using a Micromeritics Instrument Corporation (Norcross, Georgia) Accelerated Surface Area and Porosimetry (ASAP) 2020 system. Before sorption analysis, the sample was degased under high vacuum (6.7×10^{-5} bar) at a temperature of 110 ˚C overnight. The sample was backfilled with nitrogen and transferred to the analysis system. Sorption analysis was carried out at liquid nitrogen temperature (77 K). Helium was used for the free space determination, after sorption analysis, both at ambient temperature and at 77 K. Apparent surface areas were calculated from N_2 adsorption data by BET analysis.

1.2.4. Preparation of Arsenic (V) and Arsenic (III) Solutions

A weight of 0.416 g of $Na_2HAsO_4.7H_2O$ and 0.132 g of As_2O_3 were dissolved each in a 100 mL DI water to prepare 1000 ppm of As(V) and As(III), respectively. Then this solution was diluted carefully with thorough mixing to obtain a 100 ppb of arsenic solution.

1.2.5. Adsorption Test

To a 100 mL of the 100 ppb solution of arsenate and arsenite, 0.1 g, 0.08 g, or 0.06 g of the adsorbent were added under continuous stirring for 30 min. The arsenic solution was sampled carefully by filtering the adsorbent out after 30 min, 1 week, 2 weeks, 3 weeks, and 1 month. The concentration of arsenic determined by an Agilent 7500ce inductively coupled plasma-mass spectrometer (ICP-MS) was supplied by

Agilent Technologies, Inc. (Santa Clara, California). The instrument has a quadrupole mass-spectrometer with an octopole reaction system to preferentially remove polyatomic interferences. It is also equipped with an autosampler Cetac AS 520, quartz Scott type, PTFE cyclonic and quartz double-pass spray chambers, platinum or nickel cones, and quartz shielded torch.

1.2.6. Kinetics Experiment

To study the kinetics of arsenic ions adsorption on the calcined Q-3T, 0.1 g of this adsorbent was added to a number of 100 mL of 100 ppb of arsenic solutions. Then the mixtures were stirred for 30 min, 60 min, 120 min, 180 min, or 300 min. At each reaction time the As concentration was measured by ICP-MS.

1.2.7. Isotherm Experiment

Different concentrations of As(V) solution were prepared as 40, 85, 140, 180, and 230 ppb and for As(III) solutions of 40, 100, 140, 186, and 210 ppb. To each of the above solutions (100 mL), 0.1 g of adsorbent was added, and the mixture was stirred for 180 min. The equilibrium concentration (c_e) was then determined by ICP-MS.

1.2.8. Effect of pH

The effect of pH on the adsorption of As(V) and As(III) by the calcined Q-3T was studied at pH values of 4.7, 7.1, 8.8, and 9.7 for As(V) and 5.4, 8.6, 9, and 10.4 for As(III). This test was conducted using 0.1 g of the adsorbent in 100 ml of 100 ppb As(V) or As(III). The pH of the mixture was monitored by ORION digital pH meter. The pH

value was adjusted by adding 1M NaOH or 1M HNO_3 when needed.

1.2.9. Effect of Calcination Temperature

An amount of 0.1 g of uncalcined Q-3T and calcined Q-3T at 200 ˚C, 300 ˚C, 400 ˚C, or 500 ˚C were added to a 100 mL of 100 ppb of As(V) under stirring for 30 min. Then the concentration of As was determined by ICP-MS. Both uncalcined and calcined Q-3T were characterized by XRD, SEM, and BET.

1.2.10. Hybrid Adsorbent

Q-3T was mixed with diatomaceous powder that was extracted from remains of algae called diatoms that contain a lot of silica. The diatomaceous powder and the Q-3T were mixed and heated at 60 ˚C for 24 hours in an oil bath to form the hybrid adsorbent. This hybrid adsorbent was calcined at 500 ˚C and then characterized by XRD, BET, and SEM. The new hybrid adsorbent was tested for As adsorption following same method as described earlier.

1.3. Results and Discussion

1.3.1 Adsorbent Characterization

The as-synthesized Q-3T (uncalcined) showed peaks at 2Θ of 11.64˚, 23.37˚, 34.42˚, 38.55˚, 45.71˚, 60.72˚, and 62.06˚, as shown in Fig. 1(a). These peaks matched uncalcined Q-3T structure as reported in the literature [4,7,15, 17]. The calcined Q-3T at 200 ˚C showed different peaks than the uncalcined Q-3T.The peaks at 2Θ of 11.64˚and 23.37˚ in uncalcined Q-3T became broader and shifted to 13.21˚ and 26.57˚, respectively,

in the calcined Q-3T, whereas peaks at 2Θ of 34.42˚, 38.55˚, and 45.71˚ were combined in one broad peak at 35.59˚. Also, the peaks at 2Θ of 60.72˚and 62.06˚ turned into one broad peak at 60.43˚ in the calcined Q-3T, as Fig. 1(b) shows. When Q-3T was calcined at 300 ˚C, there was no difference in XRD peaks from the calcined Q-3T at 200 ˚C except that peaks are broader at the higher temperature, as presented in Fig. 1(c). At 400 ˚C and 500 ˚C of calcination, shown in Fig. 1(d and e), respectively, broad peak were observed at 2Θ of 35.27˚, corresponding to amorphous alumina. In addition, two additional peaks at 2Θ of 42.92˚ and 62.50˚ existed that corresponding to MgO (periclase). Therefore, by calcination at temperatures higher than 400 ˚C, Q-3T should be converted to Al and Mg mixed oxides.

After the adsorption of As(V) by calcined Q-3T, its layers were regenerated, and the adsorbent retrieved its original configuration before calcination as Fig. 2(a) shows. This is attributed to the rehydration during immersing in the aqueous arsenic solution, which is called “memory effect.” This is evidenced by the similarity of the XRD patterns of the adsorbent after 30 min of immersion in the aqueous solution and those of the uncalcined Q-3T except for one peak at 2Θ of 11.64˚ that was not observed after the 30 min rehydration, as presented in Fig. 2(b). This could be attributed to the fact that 30 min immersion was too short to completely regenerate the Q-3T. On the other hand, immersion of the adsorbent in the aqueous solution for a week and up to a month helped the adsorbent regain its original structure before calcination as Fig. 2(c–f) shows. To further verify this observation, the adsorbent was tested after immersion in the As(III) aqueous solution and analyzed by XRD at the same time intervals. Figure 3 proves that the adsorbent retrieved its original crystal structure after a week of the hydration and up

to three weeks. However, after 1 month of immersion the peak at 2Θ of 11.64˚ disappeared.

1.3.2 The Hybrid Adsorbent XRD

Figure 4 shows the XRD patterns of the hybrid adsorbent calcined at 500 ˚C. MgO (periclase) peaks were registered at 2Θ = 42˚ and 62˚, amorphous alumina was observed at 35.6˚, and the silica (coming from the diatomaceous powder) was clearly seen at 22˚ [18].

1.3.3 Specific Surface Area (BET)

The specific surface area of uncalcined Q-3T, calcined Q-3T at different temperatures (200, 300, 400, and 500 ˚C), Q-3T after the adsorption process, and the hybrid adsorbent were determined by BET and listed in Table 1. The uncalcined Q-3T has the smallest surface area (64.1 m^2/g), and after calcination the surface area increases with increasing the temperature. The optimum temperature is 500 ˚C at which the Q-3T has the largest surface area (193.4 m^2/g). After adsorption of As(V) and As(III) by the calcined Q-3T, its surface area decreases due to the expected filing by the adsorbate. The hybrid adsorbent has a surface area of 101.7 m^2/g.

1.3.4 Scanning Electron Microscope (SEM) and Energy Dispersive Spectroscopy (EDS)

The morphologies of Q-3T adsorbent before and after calcination and after adsorption in addition to the hybrid adsorbent were examined by SEM. Figure 5(a) shows

the morphology of as-synthesized Q-3T as clusters of particles with less porosity than calcined Q-3T, shown in Fig. 5(b). In the case of the calcined hybrid adsorbent, big clusters with few pores were seen in Fig. 5(c), whereas the hydrating calcined Q-3T for 30 min and 1 month has altered the morphology of the adsorbent, as seen in Fig. 5(d and e). The platelet-shaped structures were observed clearly after the 1 month immersion, as shown in Fig. 5(e). The particle size as determined from SEM images ranged from 12 to 56 nm for as-synthesized Q-3T and from 24 to 42 nm for the calcined Q-3T. The molar ratio of Mg:Al was found to be 2.0:1.0 in the calcined Q-3T (at 500 ˚C) as determined by EDS analysis, as presented in Fig. 6.

1.3.5 Adsorption Test

1.3.5.1. Adsorption of As(V)

Calcined Q-3T was capable of removing As(V) from aqueous solution after 30 min to 99.8%, 99.7%, and 98.4% with amount of adsorbent 0.1 g, 0.08 g, and 0.06 g, respectively. It is to be noted that these results are the average of a duplicated adsorption experiments. Figure 7 shows As(V) removal percentage (Q_t %) using 0.1 g of adsorbent (0.1 g, 0.08 g, and 0.06 g) with time as calculated by the following relationship:

$$Q_t\,\% = \frac{(c_0 - c_t)}{c_0} \times 100 \qquad (1)$$

where Q_t % is the As removal percentage at time t and c_0 and c_t are the initial concentration and concentration at time t, respectively. It was found that the As removal increases with increasing the amount of adsorbent and also the adsorbent can conserve its efficiency with time because the increasing or the decreasing in arsenic concentration from 30 min to 1 month within 5 ppb, and this is the allowed concentration limit in the

drinking water.

1.3.5.2. Adsorption of As(III)

Calcined Q-3T removed As(III) from aqueous solution after 30 min by 84.8%, 87.6%, and 95.9 % with the amount of adsorbent 0.1 g, 0.08 g, and 0.06 g, respectively. Figure 8 shows the As(III) removal percentage (Qt %) with different amounts of adsorbent (0.1 g, 0.08 g, and 0.06 g) with time. It is observed that calcined Q-3T removed As(V) better than As(III) because As(III) is more difficult to be removed than As(V) [14]. In contrast to As(V), the removal of As(III) by this adsorbent decreased with increasing the amount of this adsorbent. By increasing the contact time from 30 min to 1 month, As(III) was released back from the adsorbent to the solution (about 35% of the adsorbed As(III) was released back to the solution).

1.3.5.3. Adsorption of As from contaminated real water

In addition to the synthetic As(V) and As(III) solutions, natural As-contaminated water was examined. The arsenic concentration in this water was determined by ICP-MS to be 93.3 ppb. Two different doses of the calcined Q-3T were used: 0.1 g and 0.08 g. Doses of 0.1 g (Fig. 9) and 0.08 g of calcined Q-3T could remove about 87.6% and 81.8%, respectively, of the arsenic in this water after 30 min. The arsenic uptake increased with time. The arsenic removal percentage in natural water was different from that of the synthetic arsenic solution due to the presence of competing anions in the natural water that decreased the arsenic uptake.

1.3.6. Kinetic of As(V) and As(III) Adsorption

The adsorption capacity (q_t) of As(V) and As(III) at time t can be obtained from the following equation:

$$q_t = \frac{(c_0 - c_t)v}{m} \qquad (2)$$

where c_0 and c_t are the initial concentration and the concentration of arsenic solution at time t, respectively, in mg/L; v is the volume of arsenic solution (L); m is the mass of the adsorbent (g); and q_t is the adsorption capacity of arsenic solution at time t (mg/g).

The equilibrium adsorption capacity (q_e) of As(V) and As(III) was determined by plotting the adsorption capacity of arsenic solution at time t (mg/g) versus time t (min), as Fig. 10(a and b) shows. The q_e was obtained at 180 min for both As(V) and As(III).

The pseudo-first order, the pseudo-second order, and intraparticle diffusion models were tested against our data to determine the kinetics controlling the adsorption process.

1.3.6.1. Pseudo-first order model

$$\log(q_e - q_t) = \log q_e - \frac{k_1}{2.303} t \qquad (3)$$

where, q_e and q_t are the equilibrium adsorption capacity (mg/g) and the adsorption capacity (mg/g) at time t (min), respectively, and k_1 is the pseudo-first-order rate constant. The value of k1 can be determined from the slope of the linear plot of log (qe-qt) versus time t [19]. The equilibrium adsorption capacity (q_e) can be determined from the intercept of the same.

1.3.6.2. Pseudo-second order model

$$\frac{t}{q_t} = \frac{1}{k_2 q_e^{\,2}} + \frac{1}{q_e} t \qquad (4)$$

where, q_e and q_t are the equilibrium adsorption capacity (mg/g) and the adsorption capacity (mg/g) at time t (min), respectively, and k_2 is the pseudo-second-order rate constant of pseudo-second order, which can be determined from the intercept of the linear plot of t/q_t versus time t. The equilibrium adsorption capacity (q_e) can be determined from the slope of the same linear plot.

1.3.6.3. Intraparticle diffusion model

$$q_t = k_3 t^{1/2} + c \qquad (5)$$

where q_t is the adsorption capacity (mg/g) at time t (min). k_3 is the intraparticle-diffusion rate constant and c is also a constant and their value can be respectively determined from the slope and intercept of the linear plot of q_t versus $t^{1/2}$.

The kinetic parameters of these three models and the correlation coefficients (R^2) for the adsorption of As(V) and As(III) by calcined Q-3T are given in Table 2. It is notable that the pseudo-second order model best fitted model depending on the correlation coefficients (R^2), as shown in Fig. 11(a and b) and the agreement between q_{cal} (calculated) and q_{exp} (experimental), as presented in Table 2.

1.3.7. Adsorption Isotherms

In order to determine the adsorption of As(V) and As(III) on calcined Q-3T, the Langmuir and Freundlich models were applied to the data.

1.3.7.1. Langmuir isotherm model

This isotherm implies that one layer of adsorbate is formed on the surface of adsorbent [20]. This model is formulated as follows:

$$q = \frac{q_{\max}.b.c_e}{1+b.c_e} \qquad (6)$$

$$\frac{c_e}{q_e} = \frac{1}{q_{\max}.b} + \frac{c_e}{q_{\max}} \qquad (7)$$

where b and q_{max} are the adsorption equilibrium constant and the maximum adsorption capacity, respectively. They can be determined respectively from the intercept and slope of the linear plot of c_e/q_e versus c_e. c_e is the equilibrium adsorption concentration (mg/L), and q_e is the equilibrium adsorption capacity (mg/g).

1.3.7.2. Freundlich isotherm model

This isotherm model is applicable to multilayer adsorption on the surface of the adsorbent [19], which is expressed as:

$$q_e = K_f.c_e^{\frac{1}{n}} \qquad (8)$$

$$\log(q_e) = \log(k_f) + \frac{1}{n}\log(c_e) \qquad (9)$$

where k_f and n are the Freundlich coefficients that are defined as adsorption capacity and adsorption intensity, respectively, which can be obtained from the intercept and slope of the linear plot of log q_e against log c_e, respectively. c_e is the equilibrium adsorption concentration (mg/L), and q_e is the equilibrium adsorption capacity (mg/g).

The plots of Langmuir and Freundlich models for the adsorption of As(V) and As(III) on calcined Q-3T are shown in Fig. 12. The parameters of these two models and

the correlation coefficients (R^2) are presented in Table 3. The Langmuir model fitted the data better than the Freundlich model for As(V) and As(III) adsorption on calcined Q-3T, indicating that the adsorbate, either As(V) or As(III), forms a monolayer of on the surface of the calcined Q-3T adsorbent.

1.3.8. Hybrid Adsorbent

The hybrid adsorbent could remove 93.1% of As(V) from aqueous solution. Therefore, the calcined Q-3T is better than this hybrid adsorbent in arsenic adsorption where the former could remove 99.8% of As(V) with the same amount of adsorbent and pH. This could be attributed to the fact that the BET surface area of this hybrid adsorbent after calcination was 101.7m^2/g, which was less than that of the calcined Q-3T (193.4 m^2/g).

1.3.9. Factors Affecting As Adsorption

1.3.9.1. Effect of adsorbent dosage

Figure 13 shows that 0.1 g of calcined Q-3T offered the highest adsorption of As(V). The order of removal efficiency with respect to adsorbent dose was 0.06 g < 0.08 g < 0.1 g. However, in the case of As(III), 0.06 offered the highest As removal with the exact opposite trend to that of As(V). This is attributed to the difference in dissociation constants.

1.3.9.2. Effect of aging

As mentioned earlier, calcined Q-3T could conserve its efficiency over time up to a month as evidence by the fluctuation of As concentration in the solution within 5 ppb over the period from 30 min to a month. On the other hand, As(III) concentration increased in the solution with the time as it was released back from the adsorbent to the solution, as in Fig. 6.

1.3.9.3. Effect of pH

The pH of the solution influences the adsorption process significantly. Figure 14(a) shows that the optimal pH for As(V) adsorption by calcined Q-3T was between pH 8 and 10. Beyond this range, the adsorption of As(V) decreases as at higher pH, the OH^- ions increase in the solution; therefore, they compete with $(AsO_3)^{3-}$ ions. At lower pH, H^+ ions increase in the solution that react with nonstoichiometric Al/Mg mixed oxides, leading to form solid metal hydroxide; therefore, atmospheric CO_3^{2-} ions' adsorption are more favorable at the interlayer surface where it sterochemically fits [4]. However, the optimum pH for As(III) adsorption by calcined Q-3T was 10.4, as shown in Fig. 14(b).

1.3.9.4. Effect of calcination

Q-3T was calcined in an electric resistance furnace at temperatures of 200 ˚C, 300 ˚C, 400 ˚C, and 500 ˚C. It was found that arsenic adsorption increases with the calcination temperature, as presented in Fig. 15. It worth noting that calcination with microwave was attempted, but the XRD patterns showed no evidence of calcination.

1.4. Conclusions

Quintinite-3T (Q-3T) was synthesized and characterized by SEM, XRD, and BET. Calcined Q-3T was tested for removing As(V) and As(III) from an aqueous solution. An amount of 0.1 g of this adsorbent was found to remove 99.8 % of 100 ppb of As(V) solution and 84.8 % of 100 ppb of As(III) solution within 30 min. The optimal adsorbent dose of was 0.1 g for As(V) and 0.06 g for As(III). The BET surface area increased by increasing the calcination temperature from 200 ˚C to 500 ˚C. As a result, the maximum As adsorption was obtained by the Q-3T calcined at 500 ˚C. The As adsorption kinetics was controlled by the pseudo-second order model. The Langmuir isotherm better fitted the data than the Freundlich model. The optimal pH for As(V) and As(III) adsorption by calcined Q-3T were 9.7 and 10.4, respectively. The calcined Q-3T regained its original structure after immersion in arsenic aqueous solution due to "memory effect." The adsorbent conserved its efficiency with time until 1 month with As(V), but As(III) was released back from the adsorbent to the solution with time.

1.5. References

[1] C. Oh, S. Rhee, M. Oh, J. Park, J. Hazard. Mater., 213–214 (2012) 147–155 .

[2] T. Bujdoso, A. Patzko, Z. Galbacs, I. Dekany, Appl. Clay Sci., 44 (2009) 75–82.

[3] X. Wu, X. Tan, S. Yang, T. Wen, H. Guo, X. Wang, A. Xu, Water Res., Ahead of Print.

[4] M. Chetia, R.L. Goswamee, S. Banerjee, S. Chatterjee, L. Singh, R.B. Srivastava, H.P. Sarma, Clean Technol. Environ. Policy, 14 (2012) 21–27.

[5] N. Mahanta, S. Valiyaveettil, RSC Advances, 3 (2013) 2776–2783.

[6] E.A.M. Abdallah, G.A. Gagnon, Can. J. Civ. Eng., 36 (2009) 881–888.

[7] K.H. Goh, T.T. Lim, Z.L. Dong, Water Sci. Technol., 61 (2010) 1411–1417.

[8] A. Welch, S. Ryker, D. Helsel, P. Hamilton, Water Well J., 2001 (2001) 30–33.

[9] C. Han, H. Li, H. Pu, H. Yu, L. Deng, S. Huang, Y. Luo, Chem. Eng. J., 217 (2013) 1–9.

[10] G. Zhang, A. Khorshed, J. Paul Chen, J. Colloid Interface Sci., 397 (2013) 137–143.

[11] L. Ma, S. Tu, Desalin. Water Treat., 32 (2011) 445–452.

[12] L. Yang, Z. Shahrivari, P.K.T. Liu, M. Sahimi, T.T. Tsotsis, Ind. Eng. Chem. Res., 44 (2005) 6804–6815.

[13] K. Hristovski, P. Westerhoff, J. Crittenden, J. Hazard. Mater., 156 (2008) 604–611.

[14] D. Vu, X. Li, Z. Li, C. Wang, J. Chem. Eng. Data, 58 (2013) 71–77.

[15] N. Kondamudi, S.K. Mohapatra, M. Misra, Appl. Catal., A. , 393 (2011) 36–43.

[16] F. Li, X. Jiang, D.G. Evans, X. Duan, J. Porous Mater., 12 (2005) 55–63.

[17] N. Kondamudi, S.K. Mohapatra, M. Misra, Applied Catalysis A: General, 393 (2011) 36–43.

[18] K.-H. Goh, T.-T. Lim, Z. Dong, Water Research, 42 (2008) 1343–1368.

[19] G. Nallathambi, T. Ramachandran, V. Rajendran, R. Palanivelu, Materials Research, 14 (2011) 552–559.

[20] F. Eba, S. Gueu, A. Eya'A-Mvongbote, J. Ondo, B. Yao, J.N. Nlo, R.K. Biboutou, Int. J. Eng. Sci. Tech., 2 (2010) 5001–5016.

[21] S.J. Allen, G. McKay, J.F. Porter, J. Colloid Interface Sci., 280 (2004) 322–333.

Table 1 BET surface area.

		BET Surface Area (m^2/g)
Uncalcined		64.1
Calcined	200 ˚C	68.9
	300 ˚C	72.5
	400 ˚C	79.8
	500 ˚C	193.4
After Adsorption of As(V)	30 min	63.4
	1Week	77.7
	2Weeks	81.8
	3Weeks	76.0
	1Month	76.9
After Adsorption of As(III)	30 min	24.5
	1Week	68.7
	2Weeks	21.2
	3Weeks	61.7
	1Month	60.2
Hybrid Adsorbent		101.7

Table 2 The kinetic parameters for the adsorption of As(V) and As(III) by calcined Q-3T.

	C_0 (mg/L)	q_{exp} (mg/g)	Pseudo-first order			Pseudo-second order			Intraparticle diffusion		
			K_1	q_{cal} (mg/g)	R^2	K_2	q_{cal} (mg/g)	R^2	K_3	C	R^2
As(V)	0.0864	0.0847	0.007	0.0014	0.413	14.558	0.0848	1	0.0003	0.0809	0.469
As(III)	0.106	0.1041	0.0048	0.0013	0.096	9.492	0.1043	0.9998	0.0006	0.0961	0.431

Table 3 The isotherm parameters of the Langmuir and Freundlich models and the correlation coefficients (R^2) for the adsorption of As(V) and As(III) by calcined Q-3T.

	Langmuir			Freundlich		
	q_{max} (mg/Kg)	b (L/μg)	R^2	K_f (mg/Kg)	1/n	R^2
As(V)	178.543	2.24	0.9739	1146.04	0.3435	0.4953
As(III)	198.673	0.078	0.9936	811.895	0.5106	0.9395

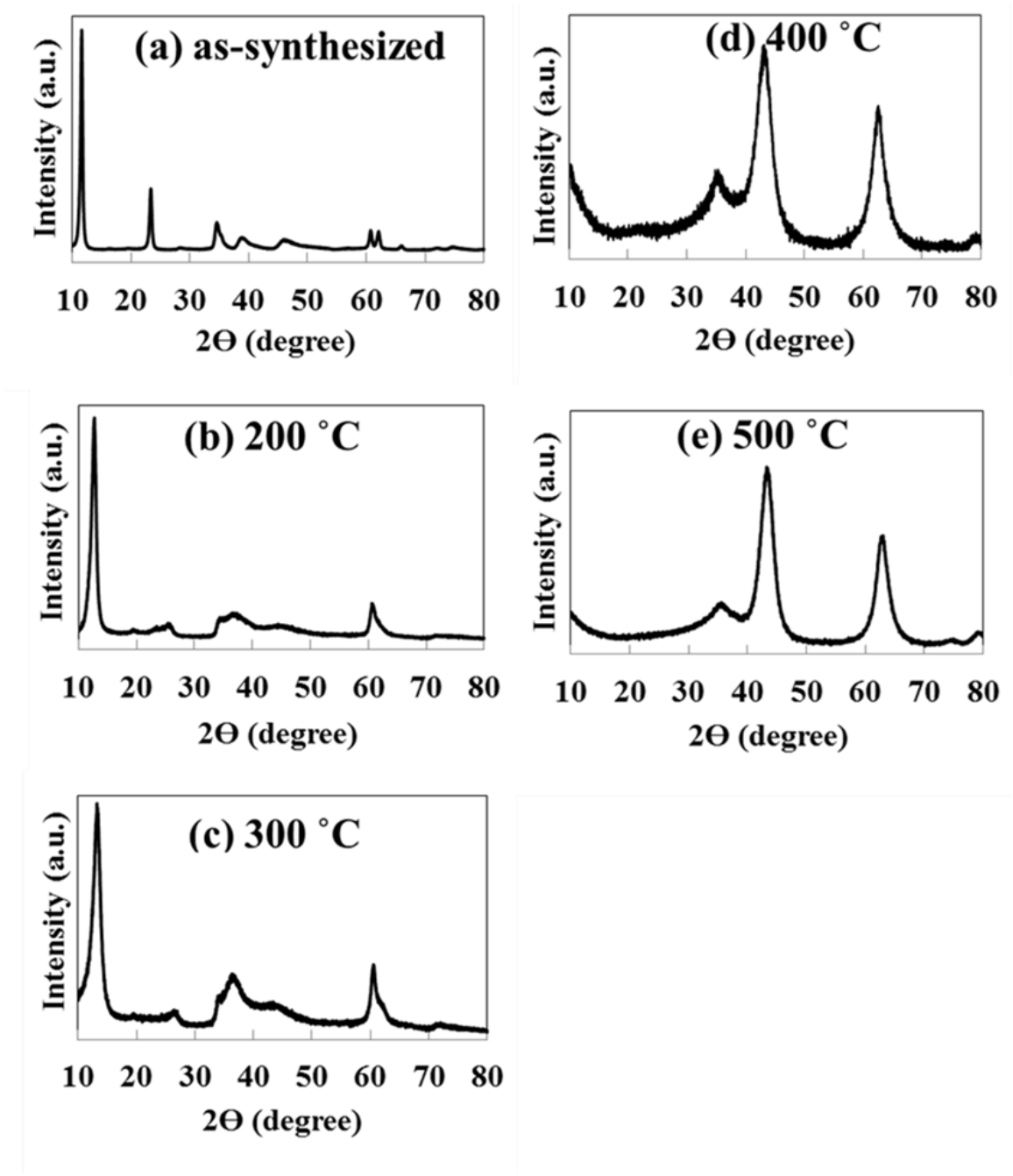

Fig. 1. XRD patterns of (a) as-synthesized Q-3T (uncalcined), (b) Q-3T calcined at 200 ˚C, (c) Q-3T calcined at 300 ˚C, (d) Q-3T calcined at 400 ˚C, and (e) Q-3T calcined at 500 ˚C.

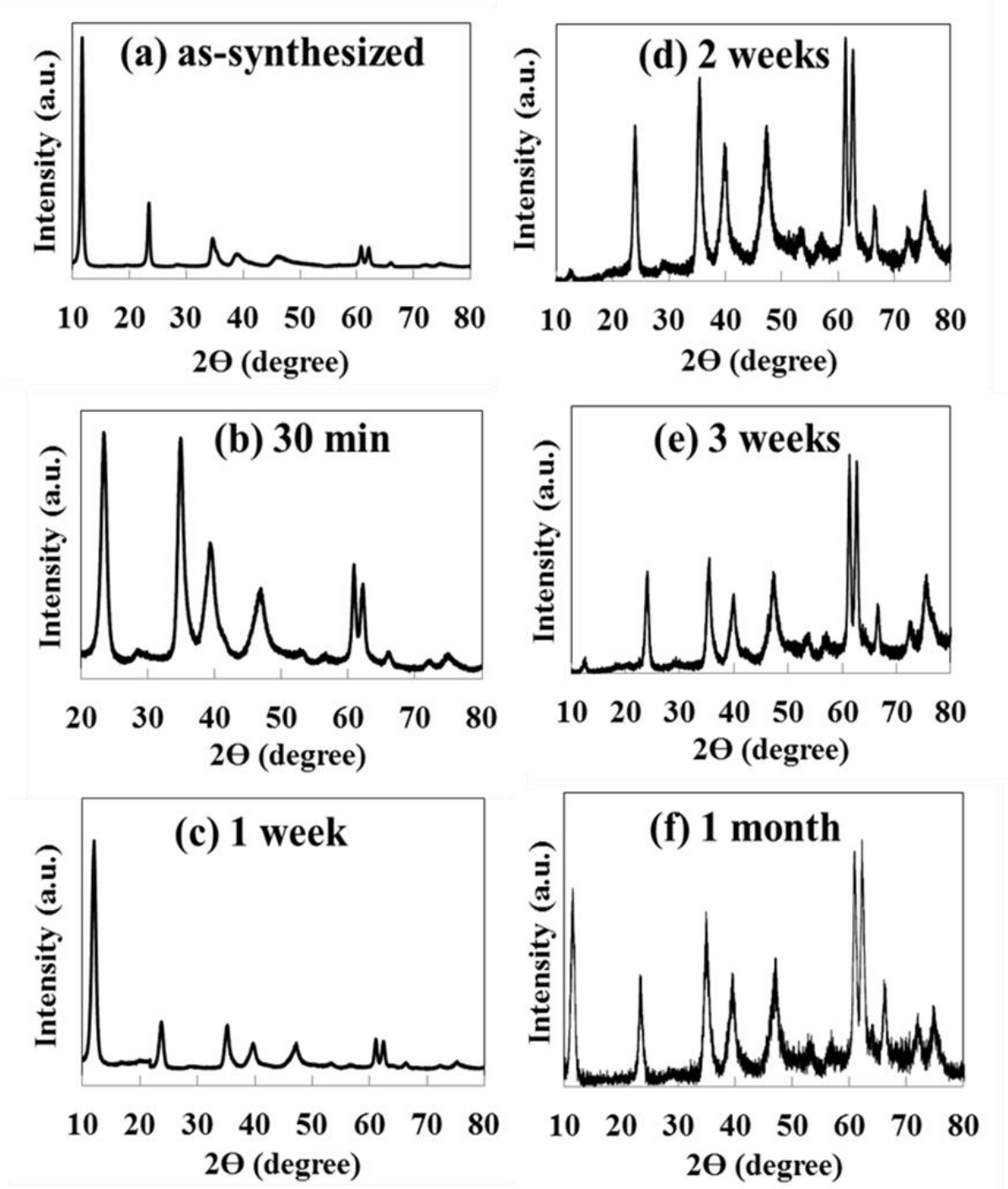

Fig. 2. XRD patterns of (a) as-synthesized Q-3T (uncalcined), (b) calcined Q-3T after 30 min of adsorption of As(V), (c) calcined Q-3T after 1 week of adsorption of As(V), (d) calcined Q-3T after 2 weeks of adsorption of As(V), (e) calcined Q-3T after 3 weeks of adsorption experiment of As(V), and (f) calcined Q-3T after 1 month of adsorption experiment of As(V).

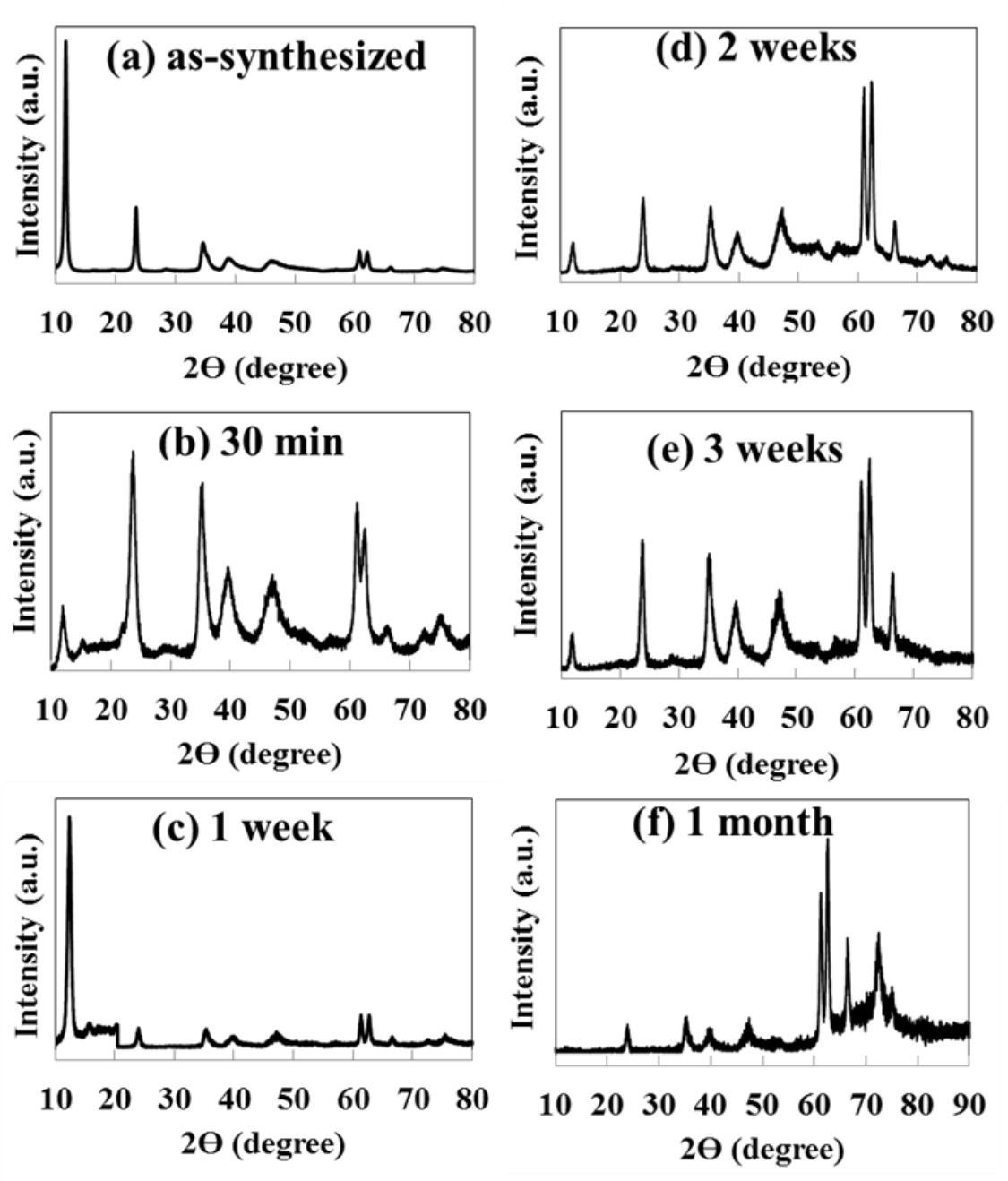

Fig. 3. XRD patterns of (a) as-synthesized Q-3T (uncalcined), (b) calcined Q-3T after 30 min of adsorption of As(III), (c) calcined Q-3T after 1 week of adsorption of As(III), (d) calcined Q-3T after 2 weeks of adsorption of As(III), (e) calcined Q-3T after 3 weeks of adsorption of As(III), and (f) calcined Q-3T after 1 month of adsorption of As(III).

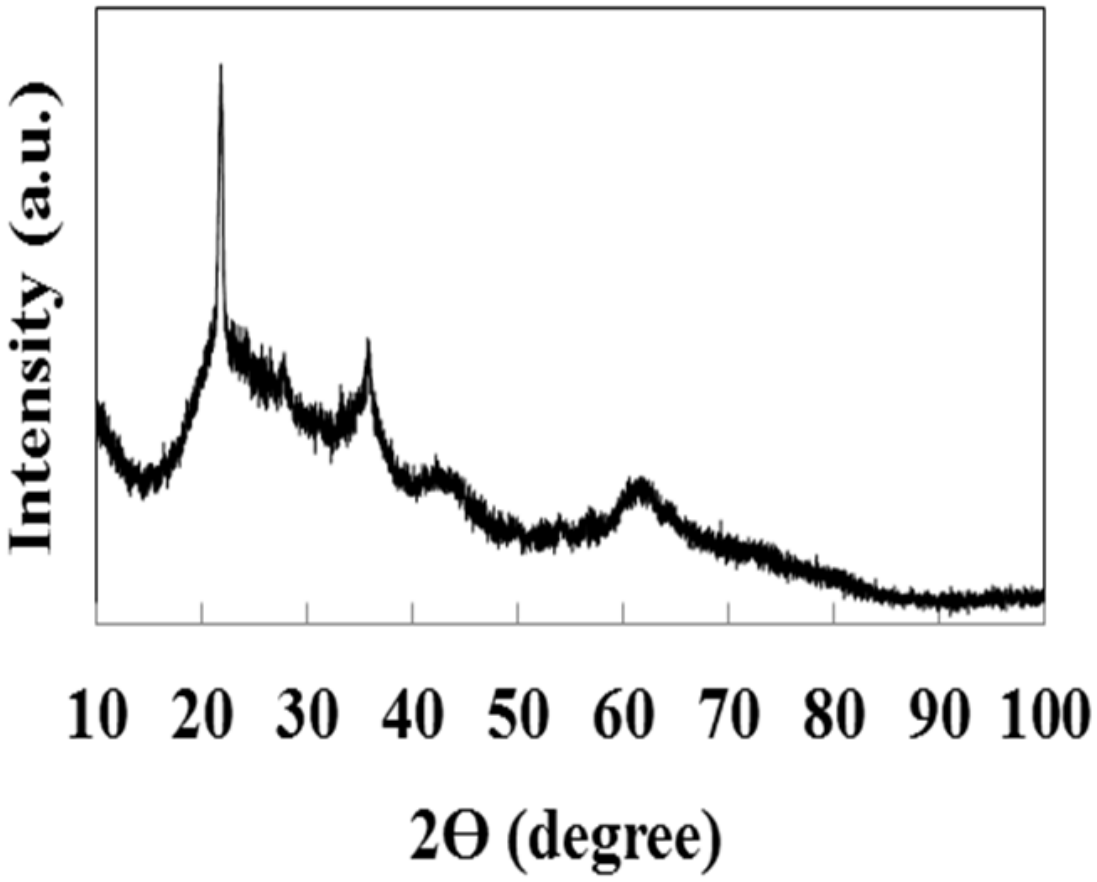

Fig. 4. XRD patterns of the calcined hybrid adsorbent.

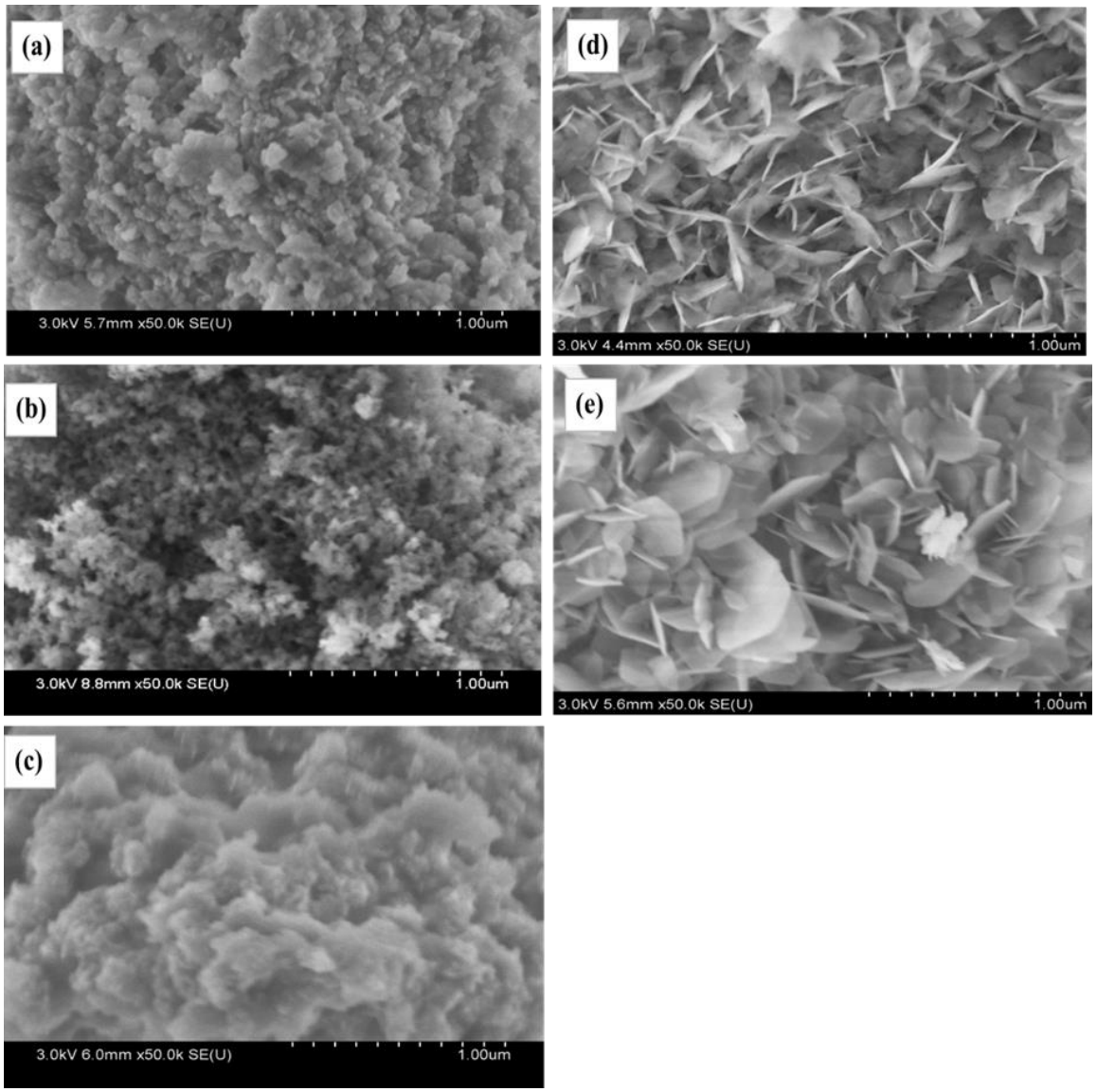

Fig. 5. SEM micrographs of (a) uncalcined Q-3T, (b) calcined Q-3T, (c) calcined hybrid adsorbent, (d) calcined Q-3T after 30 min of immersion in As solution, (e) calcined Q-3T after 1 month of immersion in As solution.

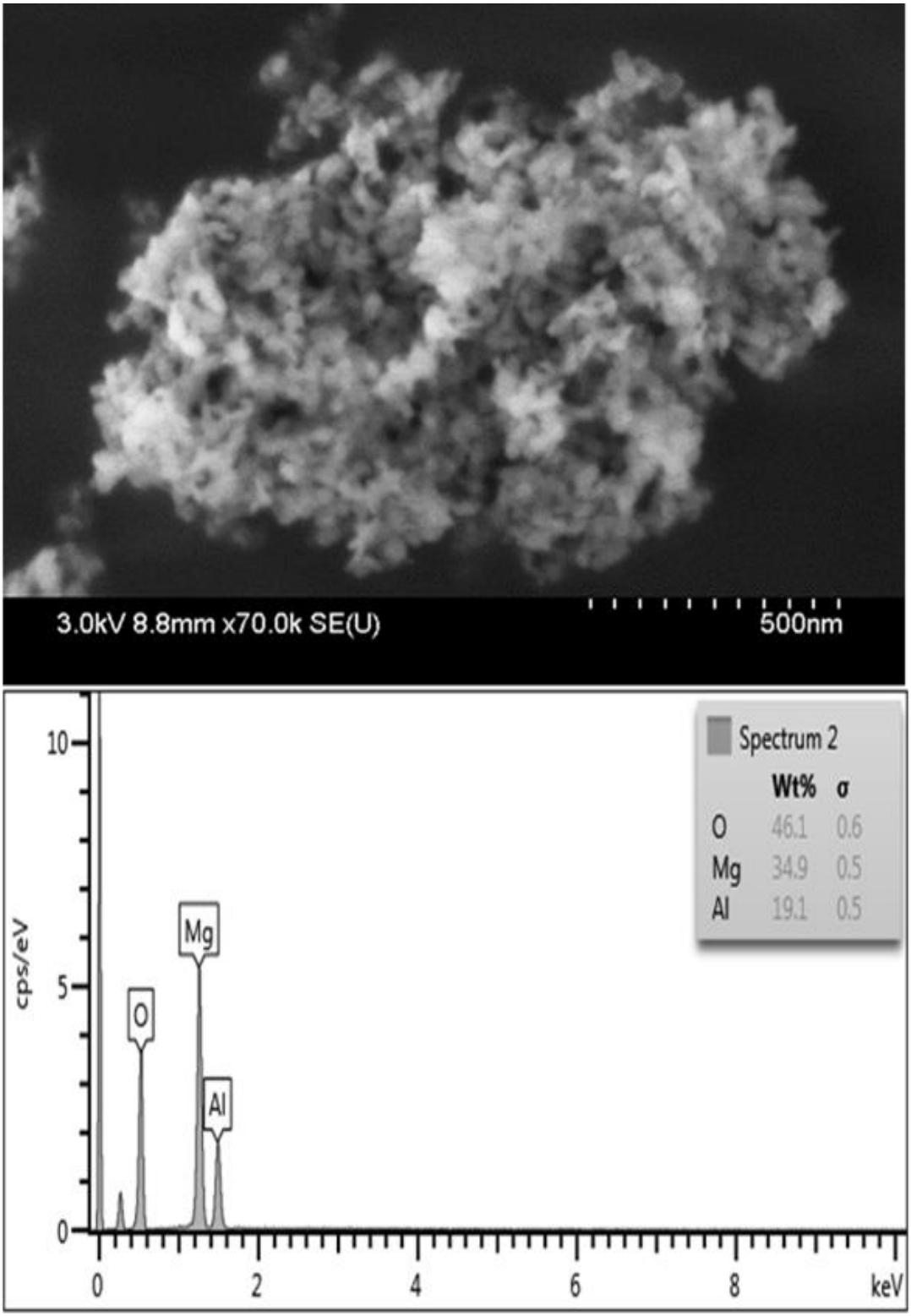

Fig. 6. SEM-EDS analysis of calcined Q-3T.

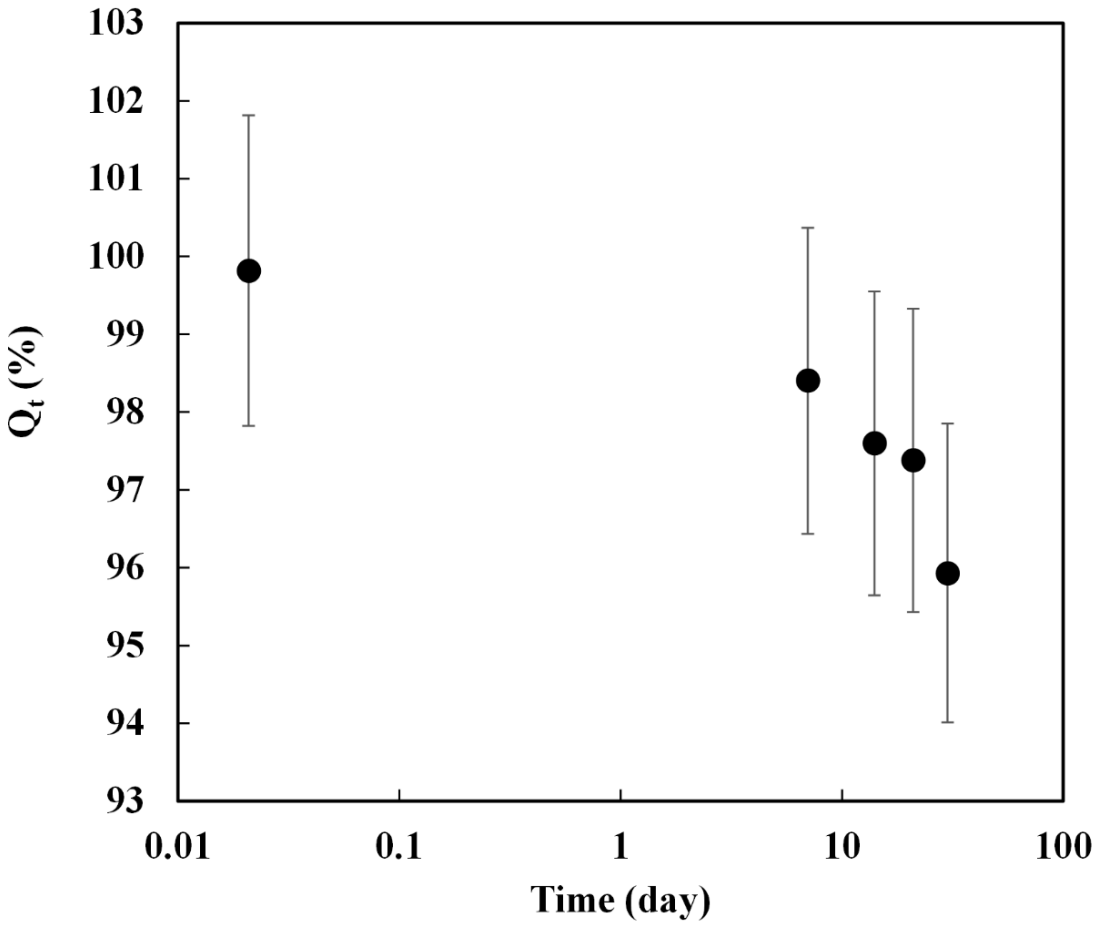

Fig. 7. Removal of As(V) with calcined Q-3T (0.1 g) from aqueous solutions with time. (Error bars represent the % deviation from the average values of at least two repeats).

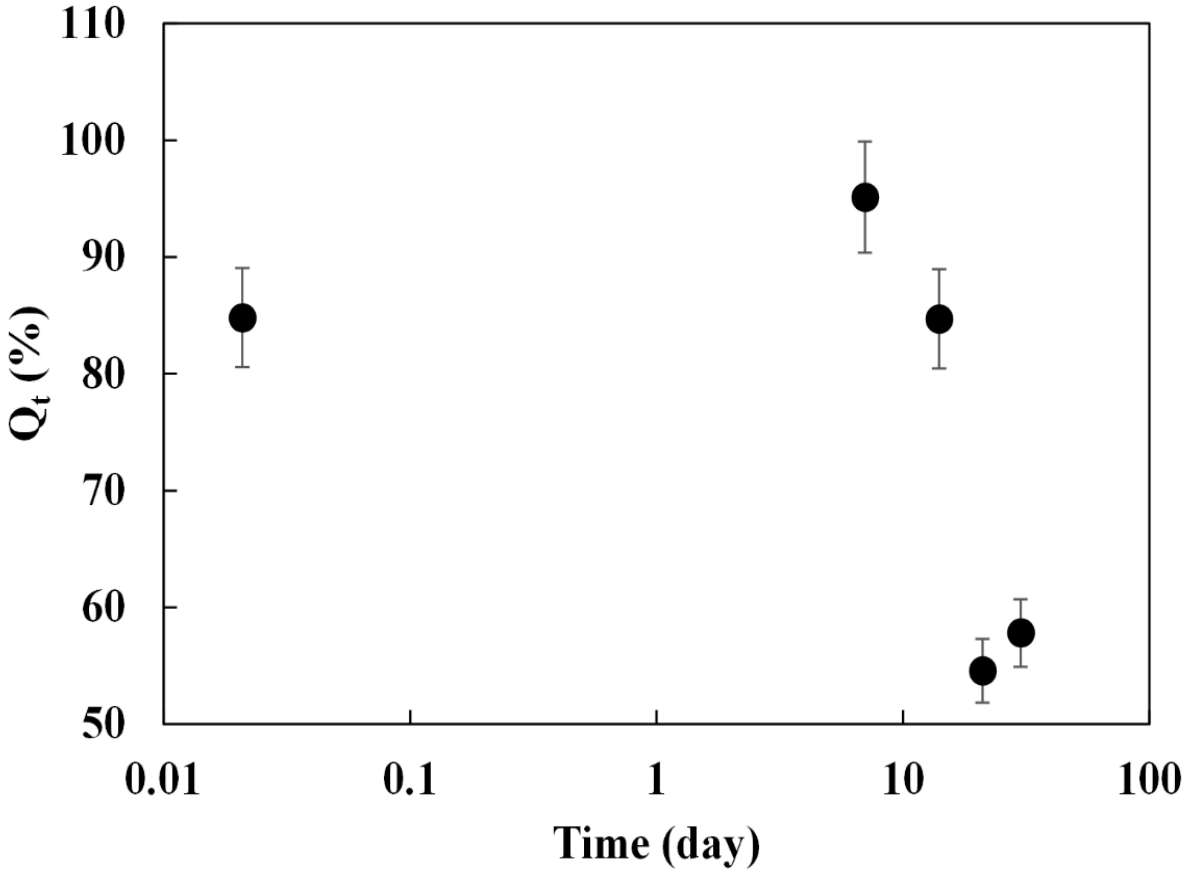

Fig. 8. Removal of As(III) with calcined Q-3T (0.1 g) from aqueous solutions with time.

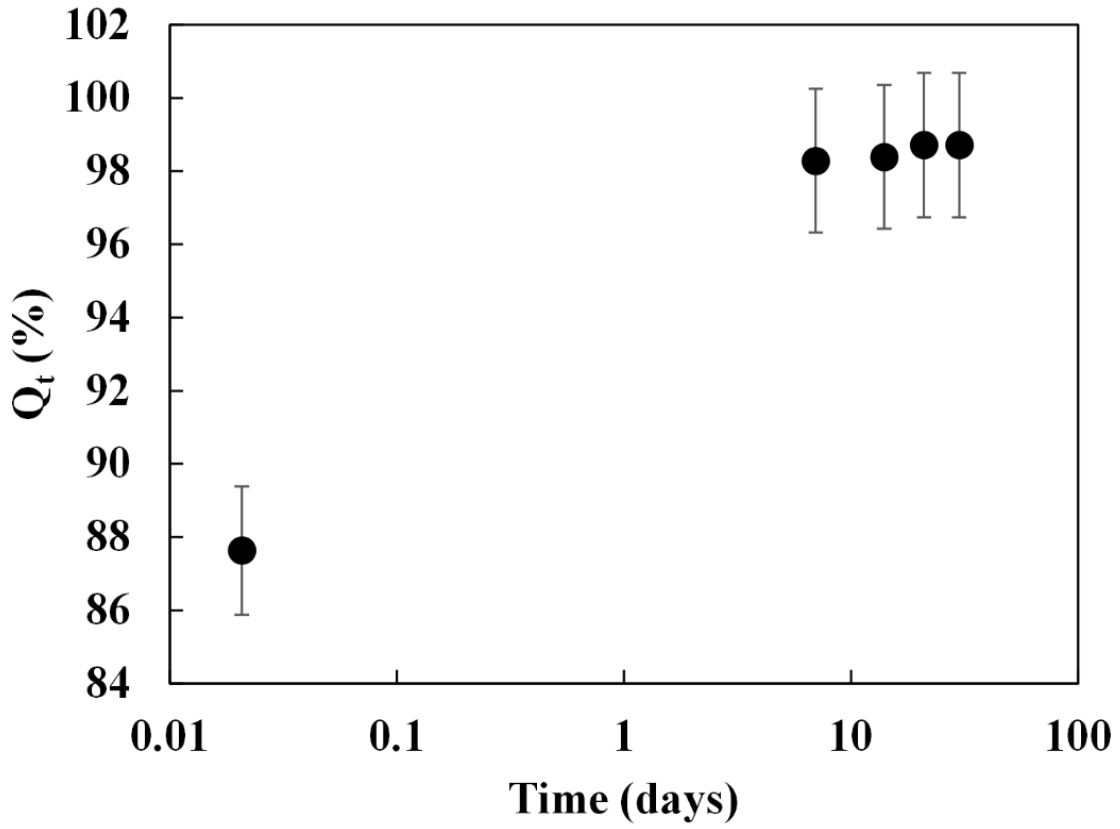

Fig. 9. Influence aging on arsenic removal using calcined Q-3T (0.1 g) from contaminated natural water with time.

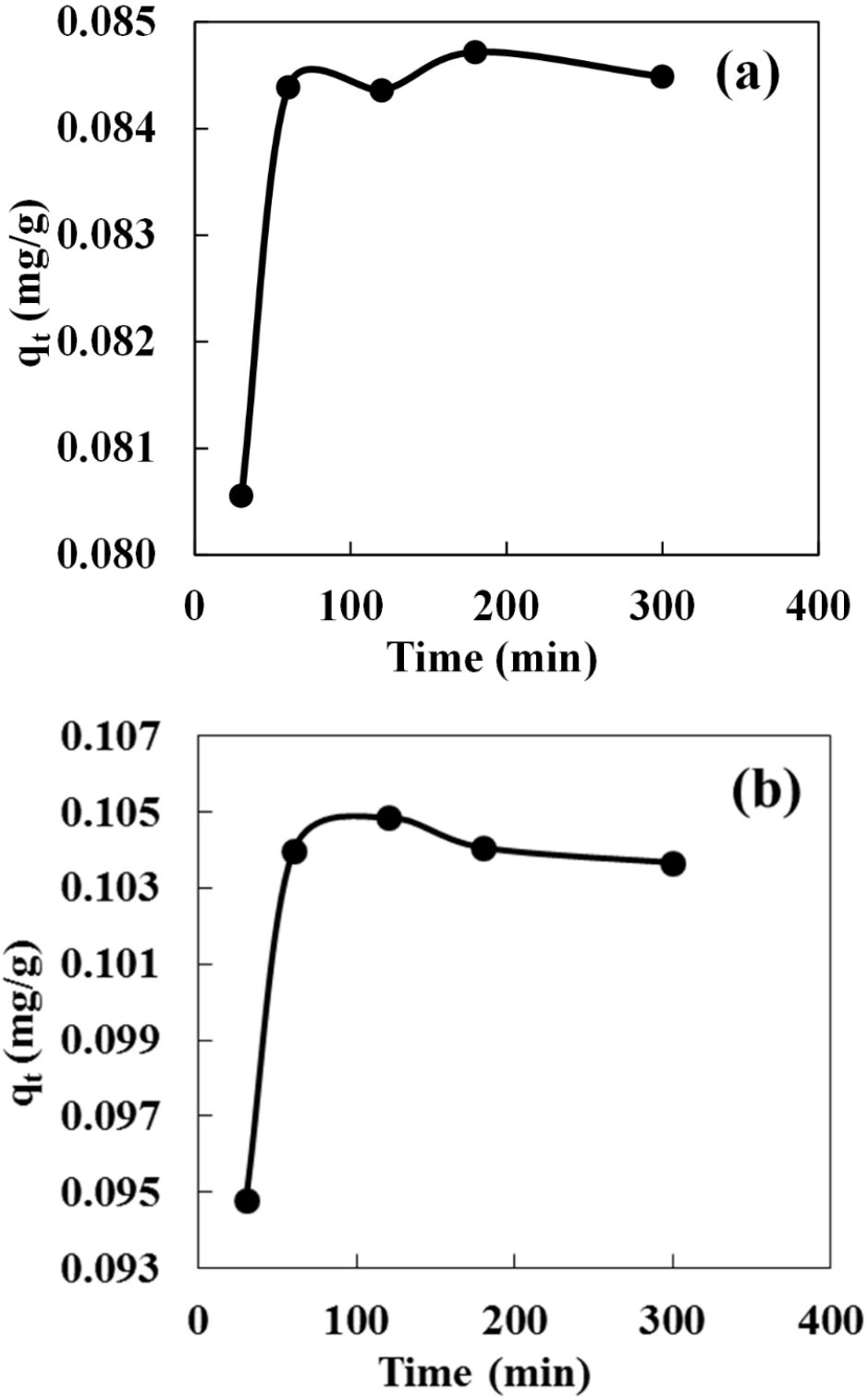

Fig. 10. The equilibrium adsorption capacity (q_e) determination for (a) As(V) and (b) As(III).

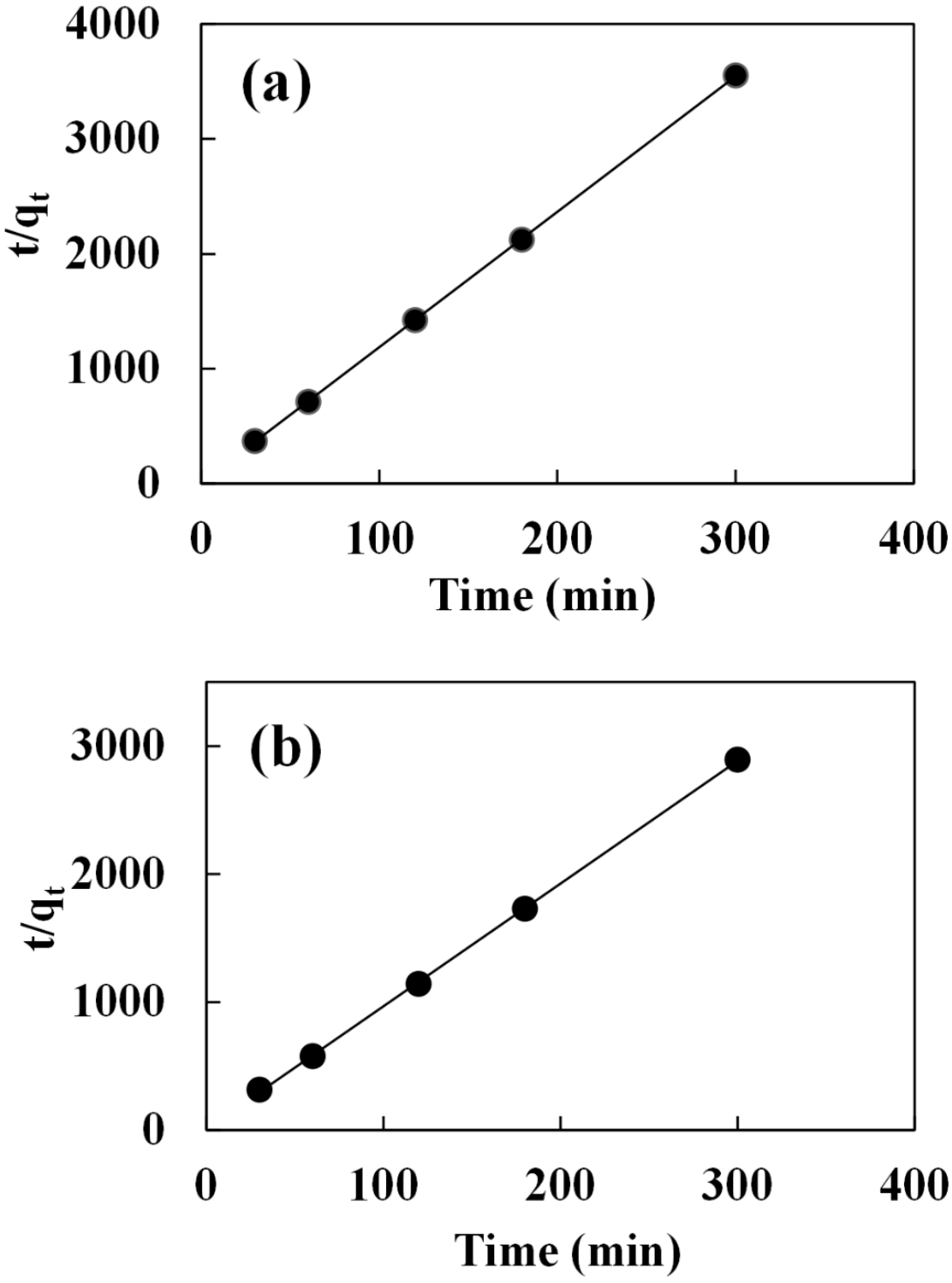

Fig. 11. The pseudo-second order plot of the adsorption of (a) As(V) and (b) As(III) by calcined Q-3T.

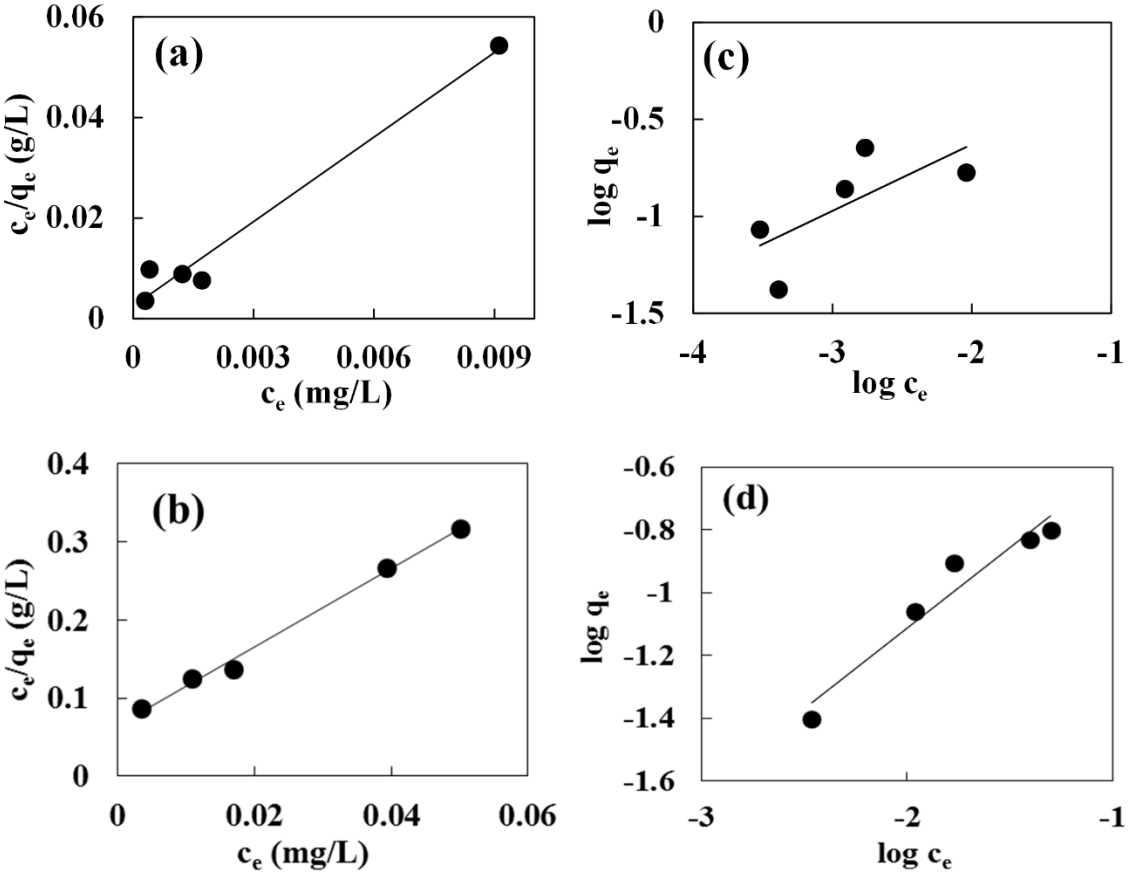

Fig. 12. The isotherm plot of (a) the Langmuir model for the adsorption of As(V), (b) the Langmuir model for the adsorption of As(III), (c) the Freundlich model for the adsorption of As(V), and (d) the Freundlich model for the adsorption of As(III).

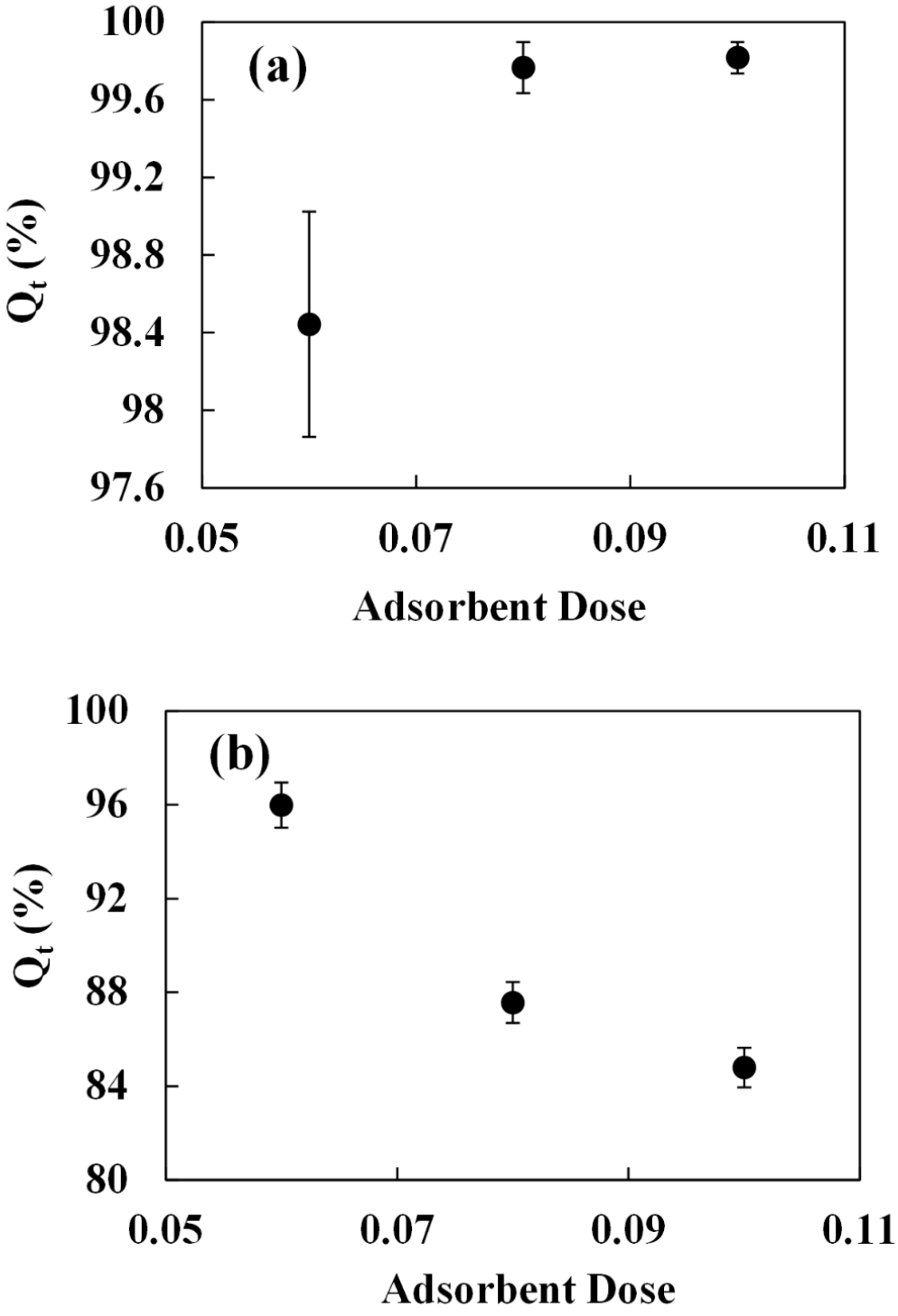

Fig. 13. The effect of adsorbent dosage on the adsorption of (a) As(V) and (b) As(III) by calcined Q-3T.

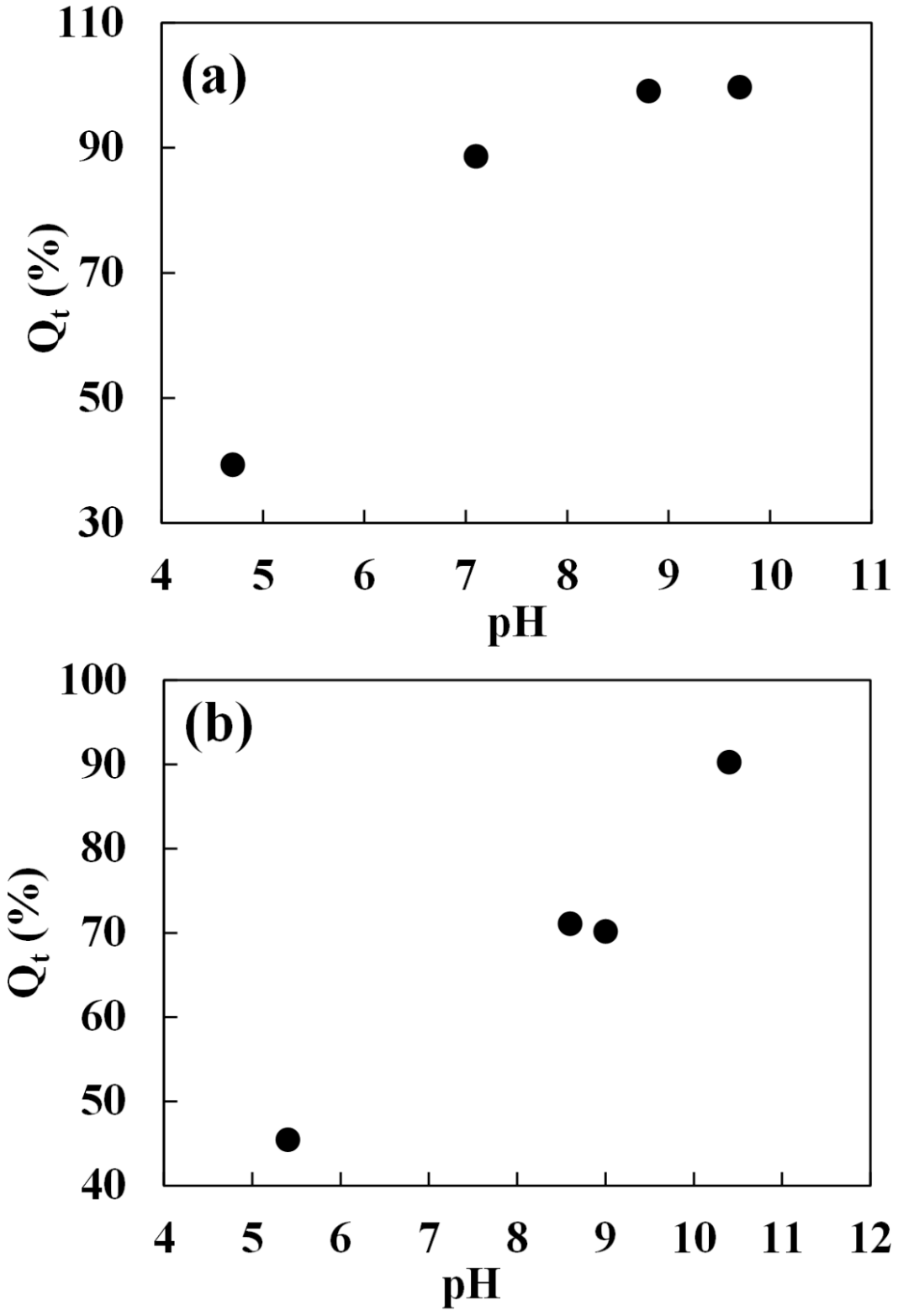

Fig. 14. The effect of pH on the adsorption of (a) As(V) and (b) As(III) by calcined Q-3T.

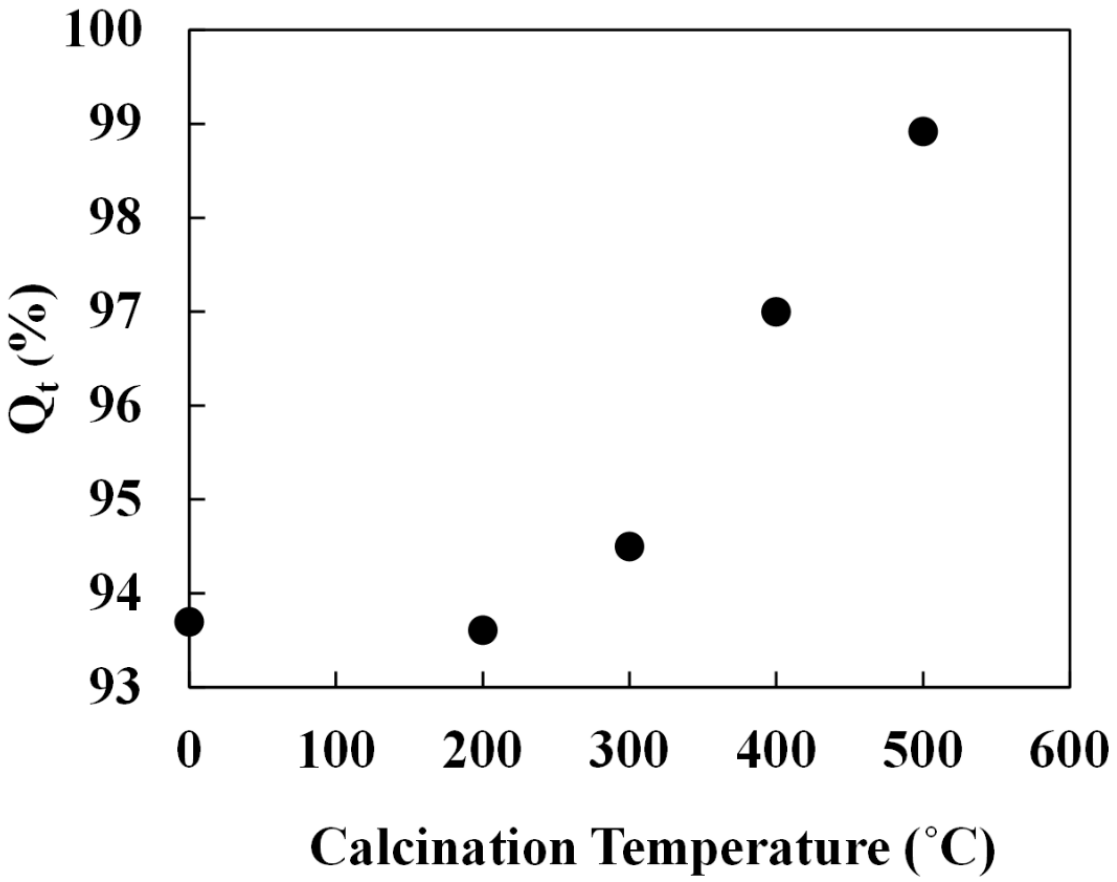

Fig. 15. The effect of calcination temperature on the adsorption of arsenic by calcined Q-3T.

CHAPTER 2

REMOVAL OF ARSENATE AND ARSENITE BY NANOCRYSTALINE CALCINED La-LDHS

2.1. Introduction

Many countries are suffering from arsenic in the drinking water all over the world, such as Bangladesh, Nepal, India, West Bengal, Argentina, Vietnam, China, Mexico, Hungary, Australia, USA, and Canada, in the form of As(III), arsenite, and As(V), arsenate [1–4]. It was reported that As(III) is more difficult to be removed from water than As(V), but fortunately As(III) exists mostly in anaerobic ground water [5]. Arsenic occuring the ground water is mainly due to minerals dissolved naturally from weathered rocks and soils over time or by human activities [6]. Arsenic is very harmful for humans, animals, and plants. Long-term exposure to As can cause hyperkeratosis, skin lesions, and various types of cancers [7], including skin and bladder cancers [8]. The Environmental Protection Agency (EPA) of the US limits arsenic concentration in drinking water to 50 ppb, and they changed this limit later to 5 ppb [8]. Many researchers have studied arsenic removal by various adsorbents, such as steel making slag [1], mesoporous alumina [9], zirconium-manganese binary hydrous oxide [10], rutile ore [11], layered double hydroxides (LDHs) [7, 12], and some nanofibers such as titanate nanofibers [13], titania nanofibers [14], and polyvinyl alcohol/Fe^{3+} nanofibers [5].

Layered double hydroxides (LDHs) are composed of metal complex hydroxides with the general formula $\{(M_{1-x}^{2+}M_x^{3+}(OH)_2)(A^{n-})_{x/n}.mH_2O\}$ [15], where M^{2+} and M^{3+} are divalent and trivalent cations, respectively. A^{n-} is an anion in the interlayer region of the brucite-like structure of LDHs [16, 17]. Therefore, LDHs are used for removing oxyanions. A good example for these LDHs is Quintinite-3T ($Mg_4Al_2(OH)_{12}CO_3•4(H_2O)$) [18], which was used for removing oxyanions such as As(V), As(III), Se(VI), Se(VI), Cr, and P. By replacing Al with La, the efficiency of adsorption of oxyanions should be changed because La is more electropositive than Al, so it should be stronger than Al in the removal of oxyanions. With calcination, La-LDHs is converted to La/Mg mixed oxides. Calcined LDHs (at about temperature 500 ˚C) are better than uncalcined LDHs in the adsorption of oxyanions [12]. The performance of calcined LDHs is higher than uncalcined LDHs [19]. This is due to the fact that by calcining LDHs at 450 to 500 ˚C, LDHs lose their original layer structure and form highly active composite metal oxides with high thermal stability, a large surface area, and a high stability against sintering even under extreme conditions [20]. In addition calcination in this temperature range increases the surface area due to the additional mesoporous regions such as channels and pores formed from the removal of water and carbon dioxide [12]. Moreover, the competing ions have a stronger effect on arsenic adsorption on the uncalcined LDHs than on the calcined LDHs [12].

In this study calcined La-LDHs adsorbent was investigated for the removal of As(V) and As(III) from water. La-LDHs adsorbent was calcined at different temperatures 200 ˚C, 300 ˚C, 400 ˚C, and 500 ˚C. The efficiency of the adsorbent for retaining As(V) and As(III) was studied from 30 min up to 1 month. The adsorbent was characterized

before and after adsorption. Arsenic was quantitatively determined by ICP-MS.

2.2. Experimental Details

2.2.1. Materials

All chemicals were used without further purification. Arsenate solution was prepared from $Na_2HAsO_4.7H_2O$ (98%) and deionized water (18.2 MΩcm). Arsenite solution was prepared from As_2O_3 (99.996%) and deionized water.

2.2.2. Adsorbent Preparation

The La/Mg solution was prepared by dissolving 56.98 g of $Mg(NO_3)_2.6H_2O$ and 48.11 g of La $(NO_3)_3.6H_2O$ in 100 mL of deionized water. The NaOH solution was prepared by dissolving 20.00 g of NaOH to 13.626 g of Na_2CO_3 in 100 mL of deionized water. Then 45 mL of Mg/La solution were added to 70 mL of NaOH solution under stirring at 400 rpm and a temperature of 60 ˚C for 24 hours in an oil bath. The precipitate was washed by deionized water, dried at 120 ˚C, and then calcined at 500 ˚C.

2.2.3. Characterization of the Adsorbent

To identify the different phases in the synthesized adsorbent (before and after calcination) the fine powder was introduced into a Rigaku MiniFlex 600 X-ray diffractometer supplied by Rigaku (The Woodlands, TX) and equipped with K_β foil filter Cu K_α radiation (λ = 1.5406 Å). The X-ray intensity was measured over 2θ (θ: diffraction angel) from 10 to 100° with a scanning rate of 0.02 °/s. To determine the morphology and particle size of the adsorbent, a Hitachi S-4800 SEM supplied by Hitachi (Tokyo, Japan)

was used. The SEM was equipped with an X-MAX tool for EDS analysis. The accelerating voltage was selected to be 10+ kV to enable the quantitative analysis of all the elements of interest.

In order to determine the average surface area of the adsorbent, volumetric N_2 sorption studies were undertaken using a Micromeritics Instrument Corporation (Norcross, Georgia) Accelerated Surface Area and Porosimetry (ASAP) 2020 system. Before sorption analysis, the sample was degased under high vacuum (6.7×10^{-5} bar) at a temperature of 110 ˚C overnight. The sample was backfilled with nitrogen and transferred to the analysis system. Sorption analysis was carried out at liquid nitrogen temperature (77 K). Helium was used for the free space determination, after sorption analysis, both at ambient temperature and at 77 K. Apparent surface areas were calculated from N_2 adsorption data by BET analysis.

2.2.4. Preparation of Arsenic (V) And Arsenic (III) Solutions

A weight of 0.416 g of $Na_2HAsO_4.7H_2O$ and 0.132 g of As_2O_3 were dissolved each in a 100 mL DI water to prepare 1000 ppm of As(V) and As(III), respectively. Then this solution was diluted carefully with thorough mixing to obtain a 100 ppb of arsenic solution.

2.2.5. Adsorption Test

To a 100 mL of the 100 ppb solution of arsenate and arsenite, 0.1 g, 0.08 g, or 0.06 g of the adsorbent were added under continuous stirring for 30 min. The arsenic solution was sampled carefully by filtering the adsorbent out after 30 min, 1 week, 2

weeks, 3 weeks, and 1 month. The concentration of arsenic was determined by an Agilent 7500ce inductively coupled plasma-mass spectrometer (ICP-MS) supplied by Agilent Technologies, Inc. (Santa Clara, California). The instrument has a quadrupole mass-spectrometer with an octopole reaction system to preferentially remove polyatomic interferences. It is also equipped with an autosampler Cetac AS 520, quartz Scott type, PTFE cyclonic and quartz double-pass spray chambers, platinum or nickel cones, and quartz shielded torch.

2.2.6. Kinetics Experiment

To study the kinetics of arsenate and arsenite adsorption on the calcined La-LDHs, 0.1 g of this adsorbent was added to a number of 100 mL of 100 ppb of arsenic solutions. Then the mixtures were stirred for 30 min, 60 min, 120 min, 180 min, 240, 300, or 360 min. At each reaction time the As concentration was measured by ICP-MS.

2.2.7. Isotherm Experiment

Different concentrations of As(V) solution were prepared as 40, 85, 100, and 230 ppb, and for As(III) solutions of 40, 100, 140, and 210 ppb were prepared. To each of the above solutions (100 mL), 0.1 g of adsorbent were added, and the mixture was stirred for 180 min. The equilibrium concentration (c_e) was then determined by ICP-MS.

2.2.8. Effect of pH on As Adsorption

The effect of pH on the adsorption of As(V) and As(III) by the calcined La-LDHs was studied at pH values of 4.5, 5.4, 8.5, and 10.5 for As(V) and 5, 6.3, 8.8, and 10.7 for

As(III). This test was conducted using 0.1 g the adsorbent in 100 ml of 100 ppb As(V) or As(III). The pH of the mixture was monitored by ORION digital pH meter. The pH value was adjusted by adding 1M NaOH or 1M HNO_3 when needed.

2.2.9. Effect of Calcination Temperature

An amount of 0.1 g of uncalcined La-LDHs and calcined La-LDHs at 200 ˚C, 300 ˚C, 400 ˚C, or 500 ˚C were added to a 100 mL of 100 ppb of As(V) under stirring for 30 min. Then the concentration of As was determined by ICP-MS. Both uncalcined and calcined La-LDHs were characterized by SEM and BET.

2.3. Results and Discussion

2.3.1. Adsorbent Characterization

2.3.1.1. XRD

The As-synthesized La-LDHs (uncalcined) showed peaks at 2Ɵ of 15.77˚, 18.55˚, 28.0˚, 38.03˚, 39.49˚, 48.54˚, 50.76˚, 55.42˚, 58.73˚, and 76.64˚ as shown in Fig. 16(a). These peaks matched the structure of La-LDHs since these peakes are for Brucite $Mg(OH)_2$ [15] and $La(OH)_3$[21] from XRD data. The XRD of calcined La-LDHs at 200 ˚C showed peaks similar to peaks of the uncalcined La-LDHs in Fig. 16(b). When La-LDHs was calcined at 300 ˚C, the XRD peaks were different from the calcined La-LDHs at 200 ˚C, as presented in Fig. 16(c). At 400 ˚C and 500 ˚C of calcination, shown in Fig. 16(d and e), respectively, peaks were observed corresponding to La_2O_3 from XRD data. In addition, two additional peaks at 2Ɵ of 42.82˚ and 62.29˚ existed that correspond to MgO (periclase) [15, 18]. Therefore, by calcination at temperatures higher than 400 ˚C,

La-LDHs should be converted to La and Mg mixed oxides.

2.3.1.2. Specific surface area (BET)

The specific surface area of uncalcined La-LDHs, calcined La-LDHs at different temperatures (200, 300, 400, and 500 ˚C), and calcined La-LDHs after the adsorption process were determined by BET and listed in Table 4. The uncalcined La-LDHs has a small surface area (86.5 m^2/g), and after calcination the surface area increases with increasing the temperature. The optimum temperature is 500 ˚C, at which the La-LDHs has the largest surface area (112.4 m^2/g). After adsorption of As(V) and As(III) by the calcined La-LDHs, its surface area decreases due to the expected filing by the adsorbate.

2.3.1.3. Scanning Electron Microscope (SEM) and
Energy Dispersive Spectroscopy (EDS)

The morphologies of La-LDHs adsorbent before and after calcination and after adsorption were examined by SEM. Figure 17(a) shows the morphology of As-synthesized La-LDHs with less porosity than calcined La-LDHs, shown in Fig. 17(b). After the adsorption, the morphology of calcined La-LDHs appeared as platelet-shaped structures after 30 min, as shown in Fig. 17(c) and after 1 month as shown in Fig. 17(d). The particle size as determined from SEM images ranged from 27 to 56 nm for As-synthesized La-LDHs and from 18 to 35 nm for the calcined La-LDHs.

The molar ratio of Mg:La was found to be 2.0:1.0 in the calcined La-LDHs (at 500 ˚C), as determined by EDS analysis.

2.3.2. Adsorption Test

2.3.2.1. Adsorption of As(V)

It was observed that calcined La-LDHs could remove As(V) from aqueous solution after 30 min to 97.9 %, 97.2 %, and 95.1 % with amount of adsorbent 0.1 g, 0.08 g, and 0.06 g, respectively. It is noted that these results are the average of a duplicated adsorption experiments.

Figure 18 shows As(V) removal percentage (Q_t %) using 0.1 g dose of adsorbent with time as calculated by the following relationship:

$$Q_t\,\% = \frac{(c_0 - c_t)}{c_0} \times 100 \qquad (10)$$

where Q_t % is the As removal percentage at time t and c_0 and c_t are the initial concentration and concentration at time t, respectively. It was found that the As removal increases with increasing of the amount of adsorbent, and also the adsorbent can conserve its efficiency with time, and the removal percentage increased with time up to 14 days, then it decreased. However, the decreasing in removal percentage of As after 14 days to 1 month within 5 ppb, and this is the allowed concentration limit in the drinking water.

2.3.2.2. Adsorption of As(III)

Calcined La-LDHs removed As(III) from aqueous solution after 30 min by 73.8%, 67.3%, and 65.2% with amount of adsorbent 0.1 g, 0.08 g, and 0.06 g, respectively. Figure 19 shows As(III) removal percentage (Qt %) with different amounts of adsorbent (0.1 g, 0.08 g, and 0.06 g) with time. It is observed that calcined La-LDHs removed As(V) better than As(III) because As(III) is more difficult to be removed than As(V) [14]. It is notable that the removal percentage increased with time up to 1 month to

be 96.4 %, 92.7 %, and 83.5 % with amount of adsorbent 0.1 g, 0.08 g, and 0.06 g, respectively.

2.3.2.3. Adsorption of As from contaminated real water

In addition to the synthetic As(V) and As(III) solutions, natural As-contaminated water was examined. The arsenic concentration in this water was determined by ICP-MS to be 93.3 ppb. Two different doses of the calcined La-LDHs were used: 0.1 g and 0.08 g. Doses of 0.1 g (Fig. 20) and 0.08 g of calcined La-LDHs could remove about 98.4 % and 97.4 %, respectively, of the arsenic in this water after 30 min. The arsenic uptake increased with time up to 14 days as in the case of the prepared arsenic solution.

2.3.3. Kinetic of As(V) and As(III) Adsorption

The adsorption capacity (q_t) of As(V) and As(III) at time t can be obtained from the following equation:

$$q_t = \frac{(c_0 - c_t)v}{m} \qquad (11)$$

where c_0 and c_t are the initial concentration and the concentration of arsenic solution at time t, respectively, in mg/L, v is the volume of arsenic solution (L), m is the mass of the adsorbent (g), and q_t is the adsorption capacity of arsenic solution at time t (mg/g).

The equilibrium adsorption capacity (q_e) of As(V) and As(III) was determined by plotting the adsorption capacity of arsenic solution (q_t) at time t (mg/g) versus time t (min), as Fig. 21(a and b) shows. The q_e was obtained at 300 min for both As(V) and As(III).

The pseudo-first order, the pseudo-second order, and intraparticle diffusion

models were tested against our data to determine the kinetics controlling the adsorption process.

2.3.3.1. Pseudo-first order model

$$\log(q_e - q_t) = \log q_e - \frac{k_1}{2.303} t \qquad (12)$$

where q_e and q_t are the equilibrium adsorption capacity (mg/g) and the adsorption capacity (mg/g) at time t (min), respectively, and k_1 is the pseudo-first-order rate constant. The value of k_1 can be determined from the slope of the linear plot of log (q_e-q_t) versus time t [22]. The equilibrium adsorption capacity (q_e) can be determined from the intercept of the same linear plot.

2.3.3.2. Pseudo-second order model

$$\frac{t}{q_t} = \frac{1}{k_2 q_e^{\,2}} + \frac{1}{q_e} t \qquad (13)$$

where, q_e and q_t are the equilibrium adsorption capacity (mg/g) and the adsorption capacity (mg/g) at time t (min), respectively, and k_2 is the pseudo-second-order rate constant of pseudo-second order, which can be determined from the intercept of the linear plot of t/q_t versus time t.

The equilibrium adsorption capacity (q_e) can be determined from the slope of the same linear plot.

2.3.3.3. Intraparticle diffusion model

$$q_t = k_3 t^{1/2} + c \qquad (14)$$

where q_t is the adsorption capacity (mg/g) at time t (min). k_3 is the intraparticle-diffusion rate constant, and c is also a constant, and their value can be, respectively, determined from the slope and intercept of the linear plot of q_t versus $t^{1/2}$.

The kinetic parameters of these three models and the correlation coefficients (R^2) for the adsorption of As(V) and As(III) by calcined La-LDHs are given in Table 5. It is notable that the pseudo-second order model is the best fitted model depending on the correlation coefficients (R^2), as shown in Fig. 22(a and b), and the agreement between q_{cal} (calculated) and q_{exp} (experimental), as presented in Table 5.

2.3.4. Adsorption Isotherms

In order to determine the adsorption of As(V) and As(III) on calcined La-LDHs, the Langmuir and Freundlich models were applied to the data.

2.3.4.1.Langmuir isotherm model

This isotherm implies that one layer of adsorbate is formed on the surface of adsorbent [23]. This model is formulated as follows

$$q = \frac{q_{max}.b.c_e}{1 + b.c_e} \qquad (15)$$

$$\frac{c_e}{q_e} = \frac{1}{q_{max}.b} + \frac{c_e}{q_{max}} \qquad (16)$$

where, b and q_{max} are the adsorption equilibrium constant and the maximum adsorption capacity, respectively. They can be determined, respectively, from the intercept and slope

of the linear plot of c_e/q_e versus c_e. c_e is the equilibrium adsorption concentration (mg/L), and q_e is the equilibrium adsorption capacity (mg/g).

2.3.4.2.Freundlich isotherm model

This isotherm model is applicable to multilayer adsorption on the surface of the adsorbent [22], which is expressed as

$$q_e = K_f . c_e^{\frac{1}{n}} \qquad (17)$$

$$\log(q_e) = \log(k_f) + \frac{1}{n}\log(c_e) \qquad (18)$$

where, k_f and n are the Freundlich coefficients that are defined as adsorption capacity and adsorption intensity, respectively, which can be obtained from the intercept and slope of the linear plot of log q_e against log c_e, respectively. c_e is the equilibrium adsorption concentration (mg/L), and q_e is the equilibrium adsorption capacity (mg/g).

The plots of the Langmuir and Freundlich models for the adsorption of As(V) and As(III) on calcined La-LDHs are shown in Fig. 23. The parameters of these two models and the correlation coefficients (R^2) are presented in Table 6. The Langmuir model fitted the data better than the Freundlich model for As(V) and As(III) adsorption on calcined La-LDHs, indicating that the adsorbate, either As(V) or As(III), forms a monolayer of on the surface of the calcined La-LDHs adsorbent.

2.3.5. Factors Affecting As Adsorption

2.3.5.1. Effect of adsorbent dosage

Figure 24 shows that 0.1 g of calcined La-LDHs offered the highest adsorption of As(V) and As(III). The order of removal efficiency with respect to adsorbent dose was 0.06 g < 0.08 g < 0.1 g.

2.3.5.2. Effect of aging

It is observed that calcined La-LDHs could conserve its efficiency over time up to a month as evidence by fluctuation of As concentration in the solution within 5 ppb over the period from 30 min to a month as shown in Fig. 18. In the case of As(III), the adsorption by calcined La-LDHs was slow, so the removal percentage increased with time up to 1 month as shown in Fig. 19.

The pH of the solution has a significant effect on the adsorption process. Figure 25(a) shows that the optimal pH for As(V) adsorption by calcined La-LDHs was between pH 7.5 and 10.5, especially at pH 8.5. Beyond this range, the adsorption of As(V) decreases as at higher pH, and the OH^- ions increase in the solution; therefore, they compete with $(AsO_3)^{-3}$ ions. At lower temperatures, H^+ ions increase in the solution, which reacts with nonstoichiometric Al/Mg mixed oxides, leading to form solid metal hydroxide; therefore, atmospheric CO_3^{-2} ions' adsorption is more favorable at the interlayer surface where they sterochemically fit [4]. However, the optimum pH for As(III) adsorption by calcined La-LDHs was 8.8, as shown in Fig. 25(b). LDHs.

2.3.5.3. Effect of calcination

La-LDHs adsorbent was calcined in an electric resistance furnace at temperatures of 200 ˚C, 300 ˚C, 400 ˚C, and 500 ˚C. It was found that arsenic adsorption increases with the calcination temperature, as presented in Fig. 26. In addition, La-LDHs calcined in the microwave, but the XRD patterns showed no evidence of calcination.

2.4. Conclusions

La-LDHs adsorbent was synthesized, calcined, and characterized by SEM, XRD, and BET. Calcined La-LDHs adsorbent was tested for removing As(V) and As(III) from aqueous solution. An amount 0.1 g of this adsorbent was found to remove 97.9 % of 100 ppb of As(V) solution and 73.8 % of 100 ppb of As(III) solution within 30 min. The optimal adsorbent dose was 0.1 g for the removal of both As(V) and As(III). The maximum As adsorption was obtained by the La-LDHs calcined at 500 ˚C because the BET surface area increased by increasing the calcination temperature from 200 ˚C to 500 ˚C. The As adsorption kinetics was controlled by the pseudo-second order model. The Langmuir isotherm better fitted the data than the Freundlich model. The optimal pH for As(V) and As(III) adsorption by calcined La-LDHs were 8.5 and 8.8, respectively. The particle size ranged from 27 to 56 nm for As-synthesized La-LDHs and from 18 to 35 nm for the calcined La-LDHs. The adsorbent conserved its efficiency with time until one month with As(V). The adsorption of As(III) increases with a long time, up to 1 month.

2.5. References

[1] C. Oh, S. Rhee, M. Oh, J. Park, J. Hazard. Mater., 213–214 (2012) 147–15.

[2] T. Bujdoso, A. Patzko, Z. Galbacs, I. Dekany, Appl. Clay Sci., 44 (2009) 75–82.

[3] X. Wu, X. Tan, S. Yang, T. Wen, H. Guo, X. Wang, A. Xu, Water Res., Ahead of Print.

[4] M. Chetia, R.L. Goswamee, S. Banerjee, S. Chatterjee, L. Singh, R.B. Srivastava, H.P. Sarma, Clean Technol. Environ. Policy, 14 (2012) 21–27.

[5] N. Mahanta, S. Valiyaveettil, RSC Advances, 3 (2013) 2776–2783.

[6] E.A.M. Abdallah, G.A. Gagnon, Can. J. Civ. Eng., 36 (2009) 881–888.

[7] K.H. Goh, T.T. Lim, Z.L. Dong, Water Sci. Technol., 61 (2010) 1411–1417.

[8] A. Welch, S. Ryker, D. Helsel, P. Hamilton, Water Well J., 2001 (2001) 30–33.

[9] C. Han, H. Li, H. Pu, H. Yu, L. Deng, S. Huang, Y. Luo, Chem. Eng. J., 217 (2013) 1–9.

[10] G. Zhang, A. Khorshed, J. Paul Chen, J. Colloid Interface Sci., 397 (2013) 137–143.

[11] L. Ma, S. Tu, Desalin. Water Treat., 32 (2011) 445–452.

[12] L. Yang, Z. Shahrivari, P.K.T. Liu, M. Sahimi, T.T. Tsotsis, Ind. Eng. Chem. Res., 44 (2005) 6804–6815.

[13] K. Hristovski, P. Westerhoff, J. Crittenden, J. Hazard. Mater., 156 (2008) 604–611.

[14] D. Vu, X. Li, Z. Li, C. Wang, J. Chem. Eng. Data, 58 (2013) 71–77.

[15] L. Yan, J. Zhuang, X. Sun, Z. Deng, Y. Li, Mater. Chem. Phys., 76 (2002) 119–122.

[16] F. Delorme, A. Seron, A. Gautier, C. Crouzet, J Mater Sci, 42 (2007) 5799–5804.

[17] J. Shibata, N. Murayama, Publ. Australas. Inst. Min. Metall., 7/2010 (2010) 389–394.

[18] N. Kondamudi, S.K. Mohapatra, M. Misra, Appl. Catal., A. , 393 (2011) 36–43.

[19] X.-Y. Yu, T. Luo, Y. Jia, R.-X. Xu, C. Gao, Y.-X. Zhang, J.-H. Liu, X.-J. Huang, Nanoscale, 4 (2012) 3466–3474.

[20] F. Li, X. Jiang, D.G. Evans, X. Duan, J. Porous Mater., 12 (2005) 55–63.

[21] Q. Li, J. Ni, Y. Wu, Y. Du, W. Ding, S. Geng, J. Rare Earth, 29 (2011) 416–419.

[22] F. Eba, S. Gueu, A. Eya'A-Mvongbote, J. Ondo, B. Yao, J.N. Nlo, R.K. Biboutou, Int. J. Eng. Sci. Tech., 2 (2010) 5001–5016.

[23] S.J. Allen, G. McKay, J.F. Porter, J. Colloid Interface Sci., 280 (2004) 322–333.

Table 4 BET surface area.

		BET Surface Area (m^2/g)
Uncalcined		86.5
Calcined	200 ˚C	85.0
	300 ˚C	91.7
	400 ˚C	87.5
	500 ˚C	112.4
After Adsorption of As(V)	30 min	52.0
	1Week	56.3
	2Weeks	49.8
	3Weeks	47.8
	1Month	56.2
After Adsorption of As(III)	30 min	60.1
	1Week	63.4
	2Weeks	54.8
	3Weeks	49.0
	1Month	55.7

Table 5 The kinetic parameters for the adsorption of As(V) and As(III) by calcined La-LDHs.

	C_0 (mg/L)	q_{exp} (mg/g)	Pseudo-first order			Pseudo-second order			Intraparticle diffusion		
			K_1	q_{cal} (mg/g)	R^2	K_2	q_{cal} (mg/g)	R^2	K_3	c	R^2
As(V)	0.0864	0.0837	0.0295	0.043	0.829	2.523	0.0842	0.9991	0.0005	0.0737	0.64
As(III)	0.1062	0.0869	0.0152	0.027	0.901	0.8644	0.092	0.9989	0.0026	0.0532	0.75

Table 6 The isotherm parameters of the Langmuir and Freundlich models and the correlation coefficients (R^2) for the adsorption of As(V) and As(III) by calcined La-LDHs.

	Langmuir			Freundlich		
	q_{max} (mg/Kg)	b (L/μg)	R^2	K_f (mg/Kg)	1/n	R^2
As(V)	106.644	2.23	0.8645	19.002	-0.2338	0.1816
As(III)	211.247	0.097	0.9826	923.847	0.4989	0.9148

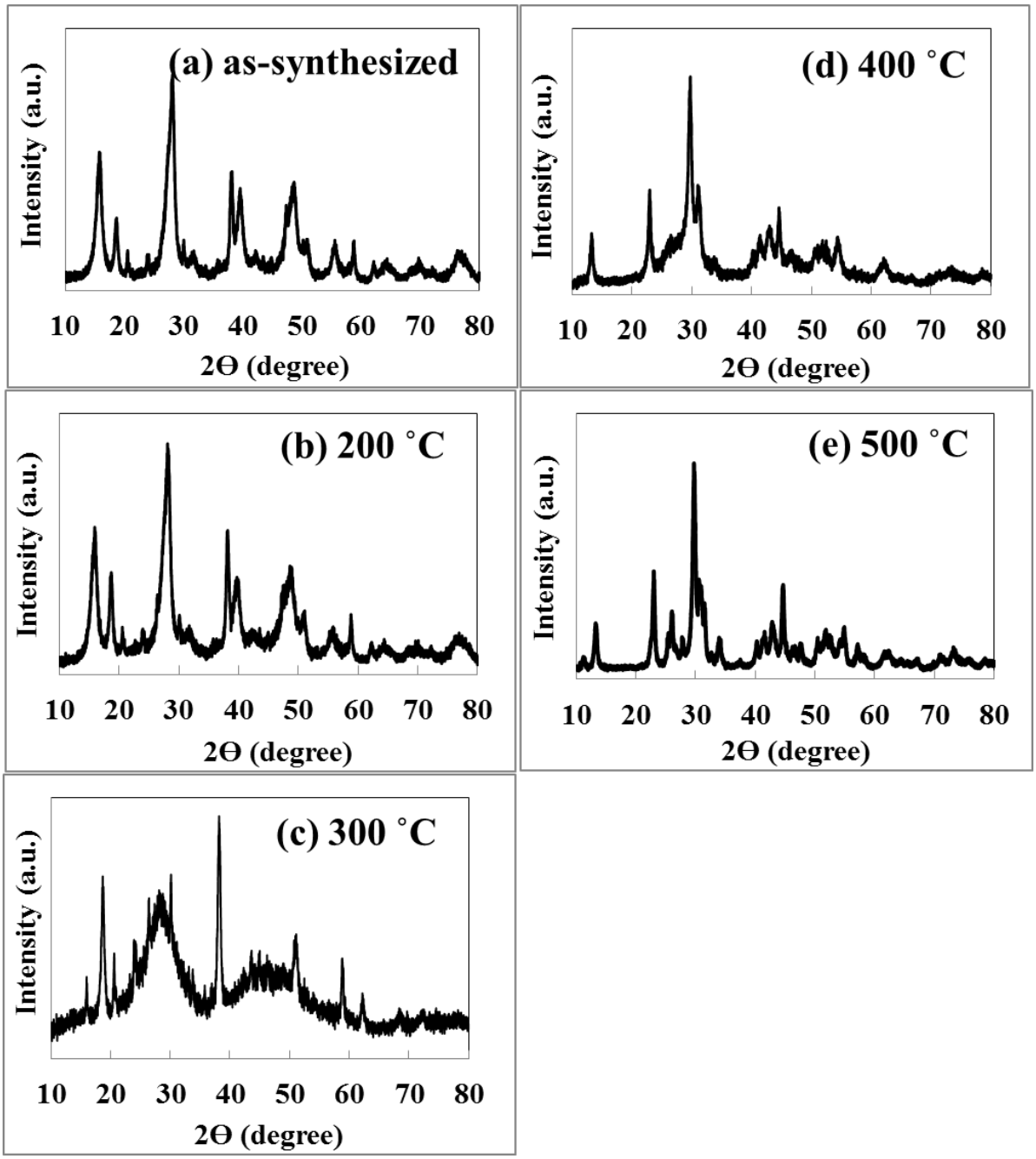

Fig. 16. XRD patterns of (a) As-synthesized La-LDHs (uncalcined), (b) La-LDHs calcined at 200 ˚C, (c) La-LDHs calcined at 300 ˚C, (d) La-LDHs calcined at 400 ˚C, and (e) La-LDHs calcined at 500 ˚C.

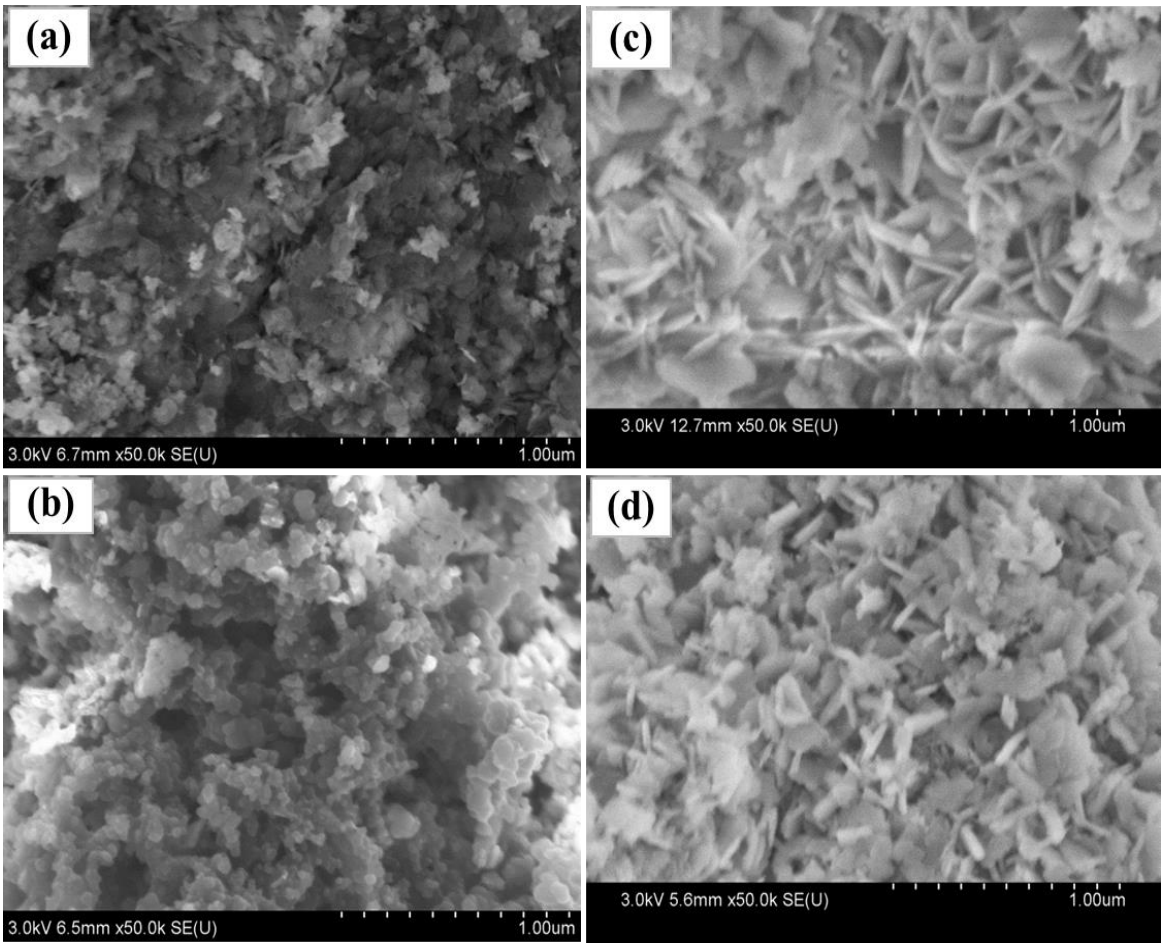

Fig. 17. SEM micrographs of (a) uncalcined La-LDHs, (b) calcined La-LDHs, (c) calcined La-LDHs after 30 min of immersion in As solution, (d) calcined La-LDHs after 1 month of immersion in As solution.

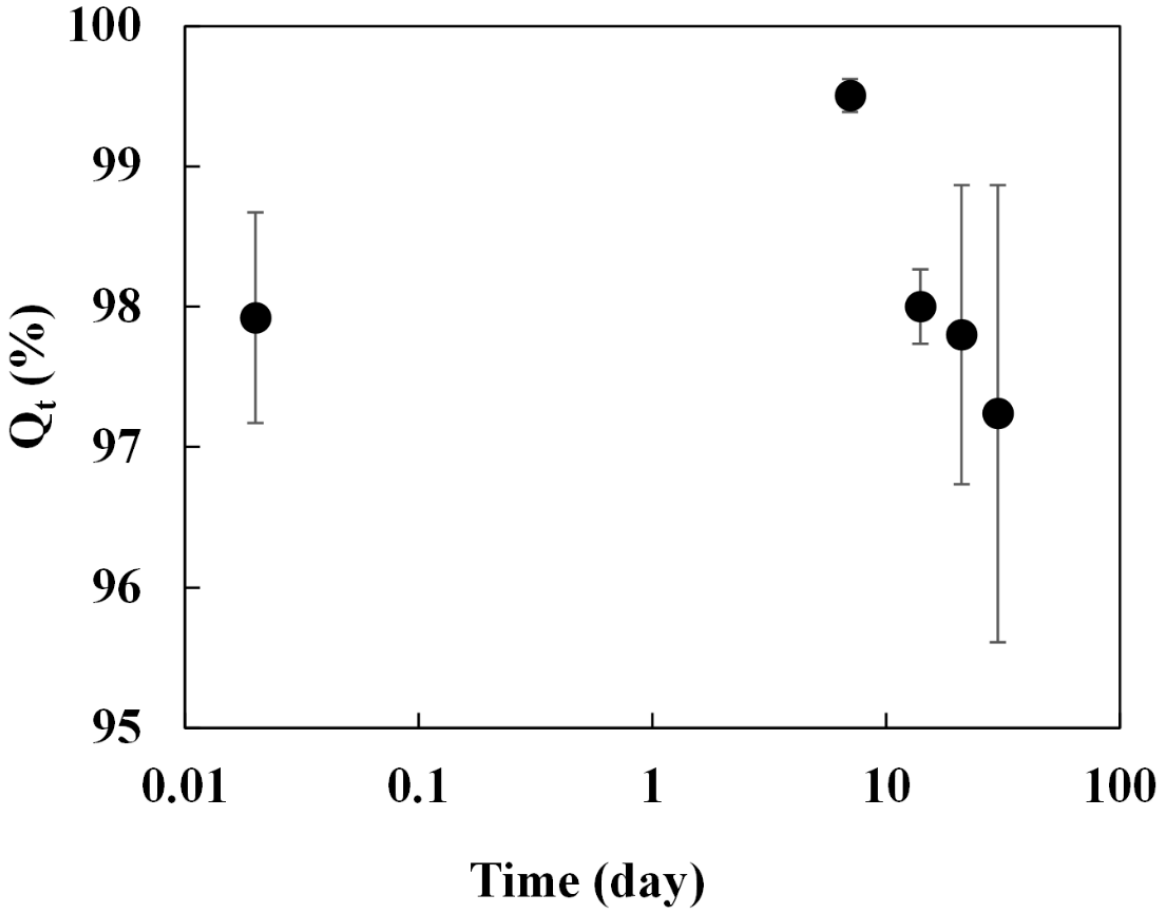

Fig. 18. Removal of As(V) using 0.1 g of calcined La-LDHs on from aqueous solutions with time.

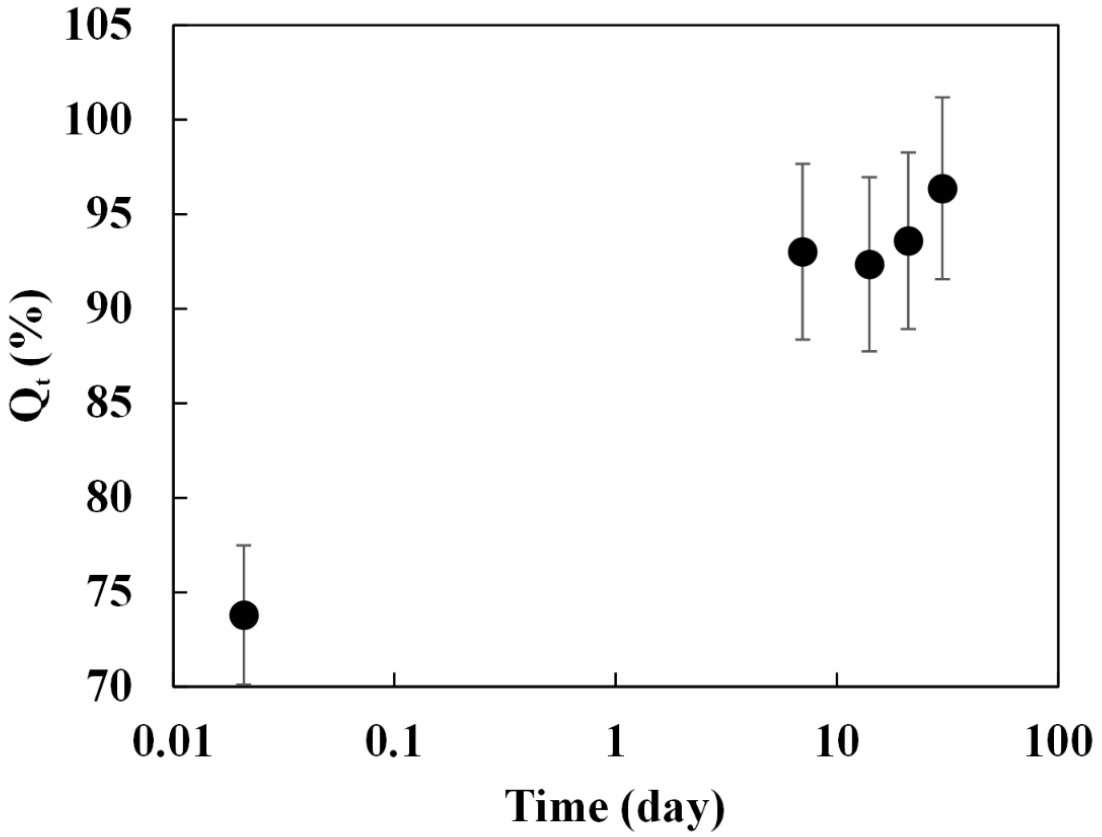

Fig. 19. Removal of As(III) using 0.1 g of calcined La-LDHs on from aqueous solutions with time.

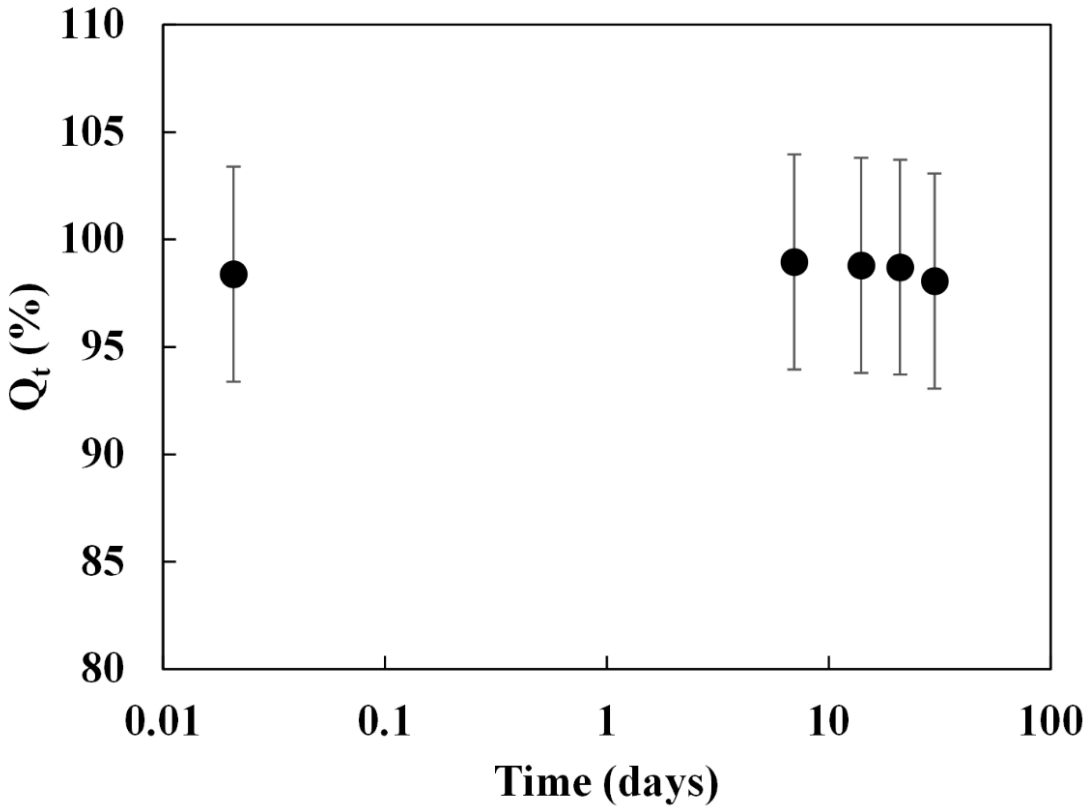

Fig. 20. Removal of As(III) using 0.1 g of calcined La-LDHs on contaminated natural water with time.

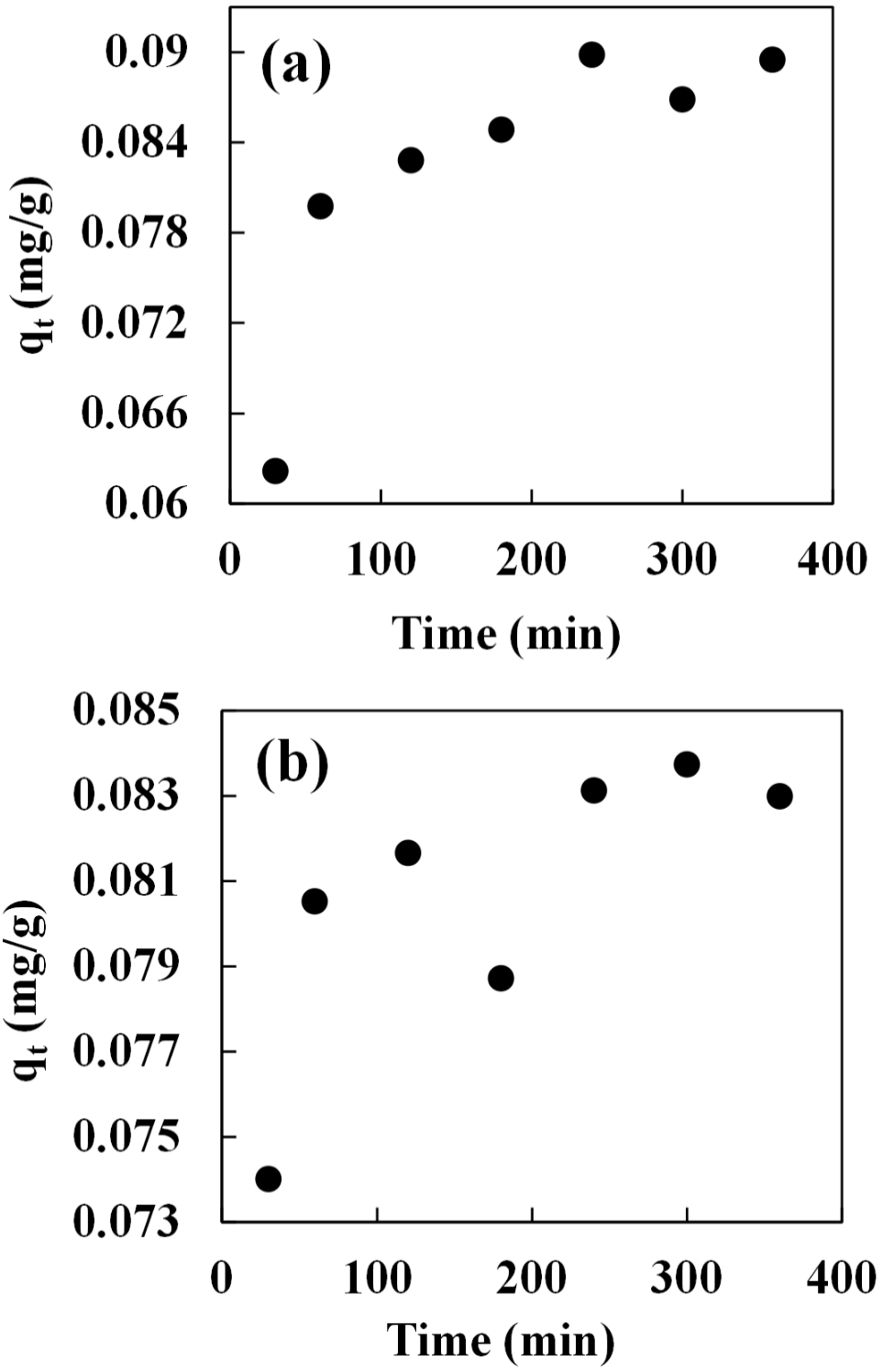

Fig. 21. The equilibrium adsorption capacity (q_e) determination for (a) As(V) and (b) As(III).

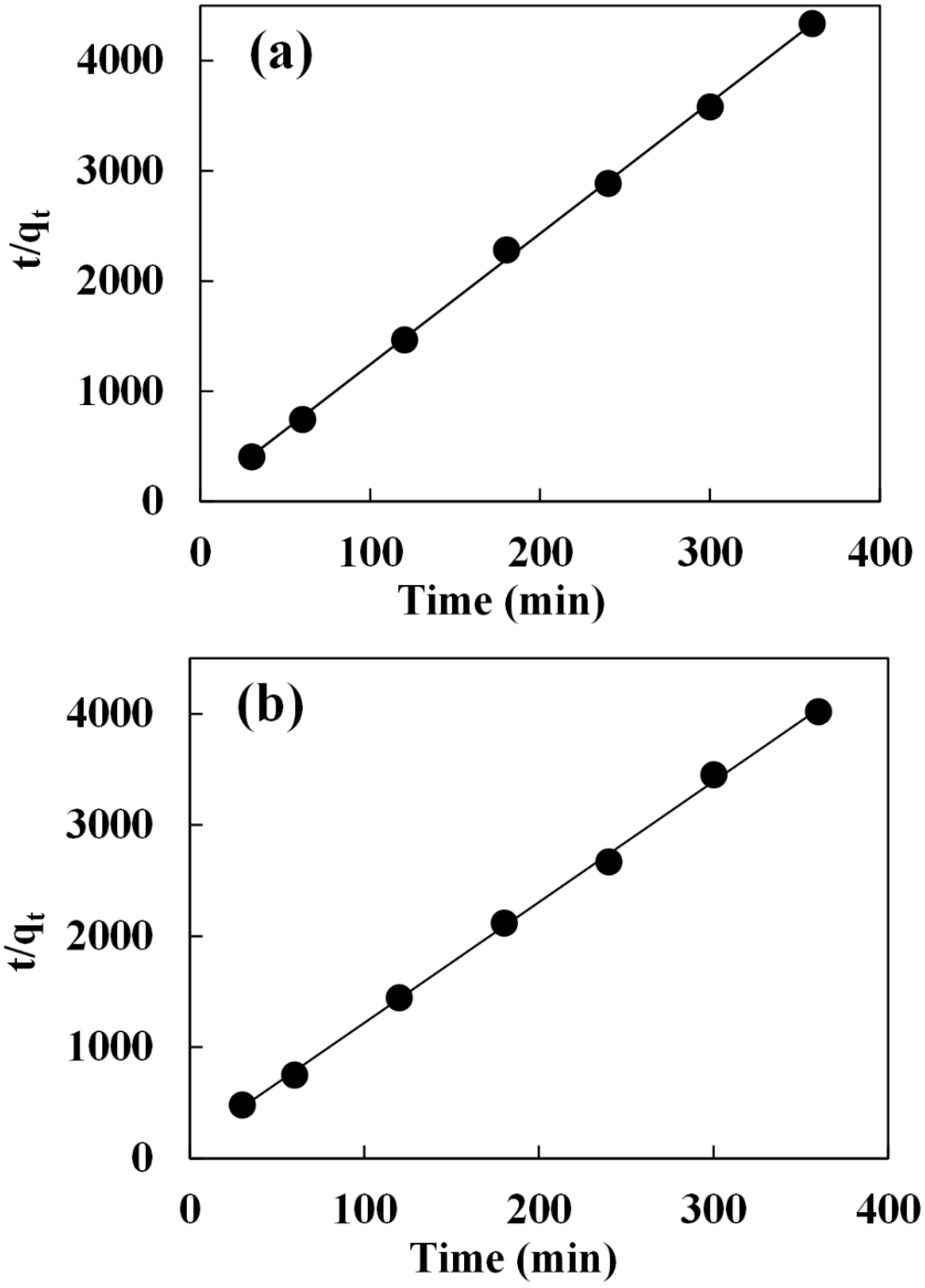

Fig. 22. The pseudo-second order plot of the adsorption of (a) As(V) and (b) As(III) by calcined La-LDHs.

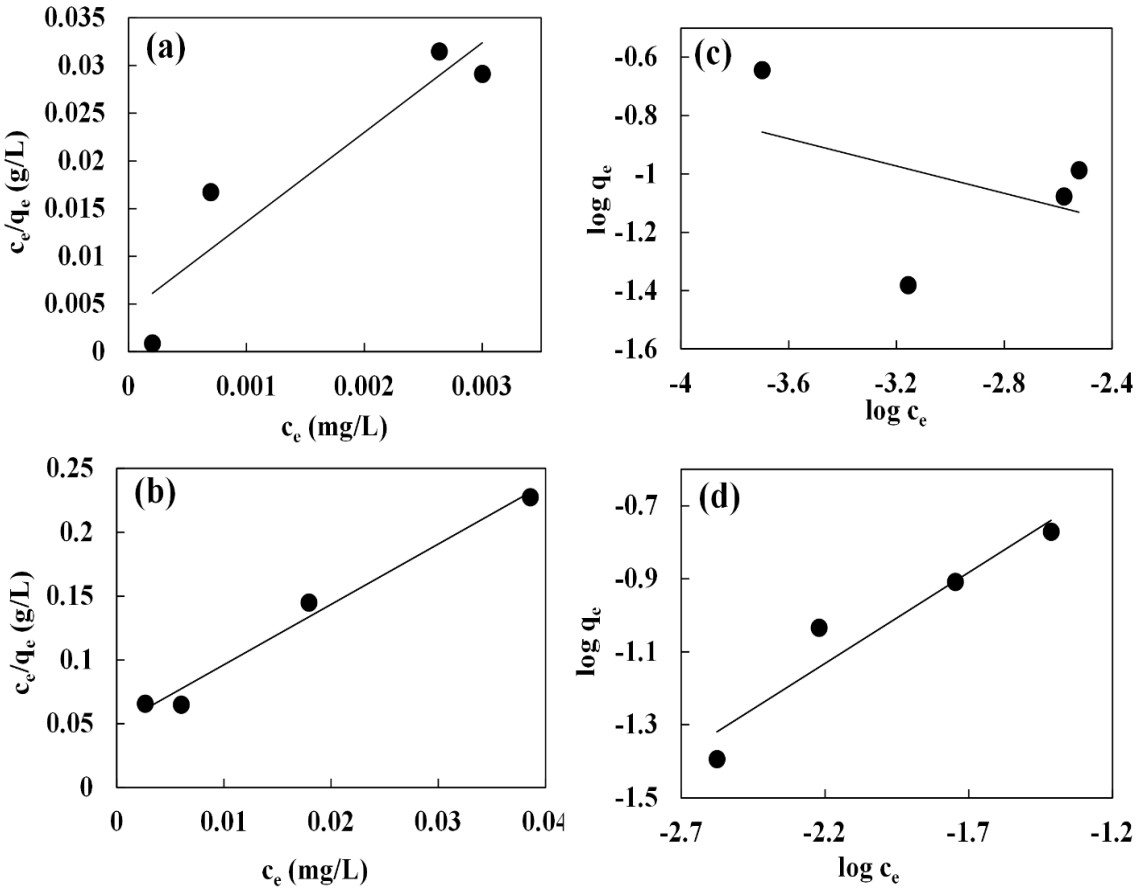

Fig. 23. The isotherm plot of (a) the Langmuir model for the adsorption of As(V), (b) the Langmuir model for the adsorption of As(III), (c) the Freundlich model for the adsorption of As(V), and (d) the Freundlich model for the adsorption of As(III).

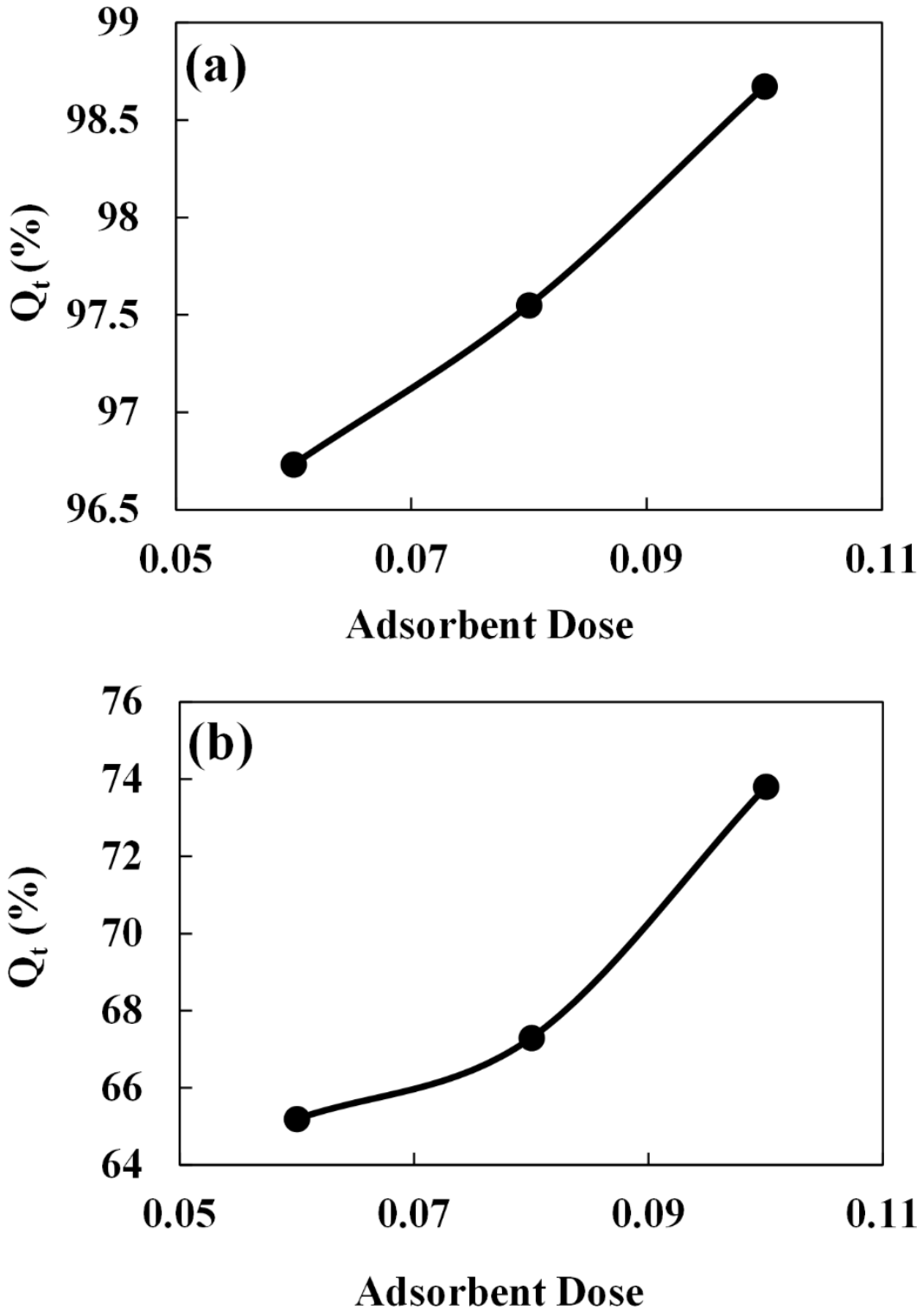

Fig. 24. The effect of adsorbent dosage on the adsorption of (a) As(V) and (b) As(III) by calcined La-LDHs.

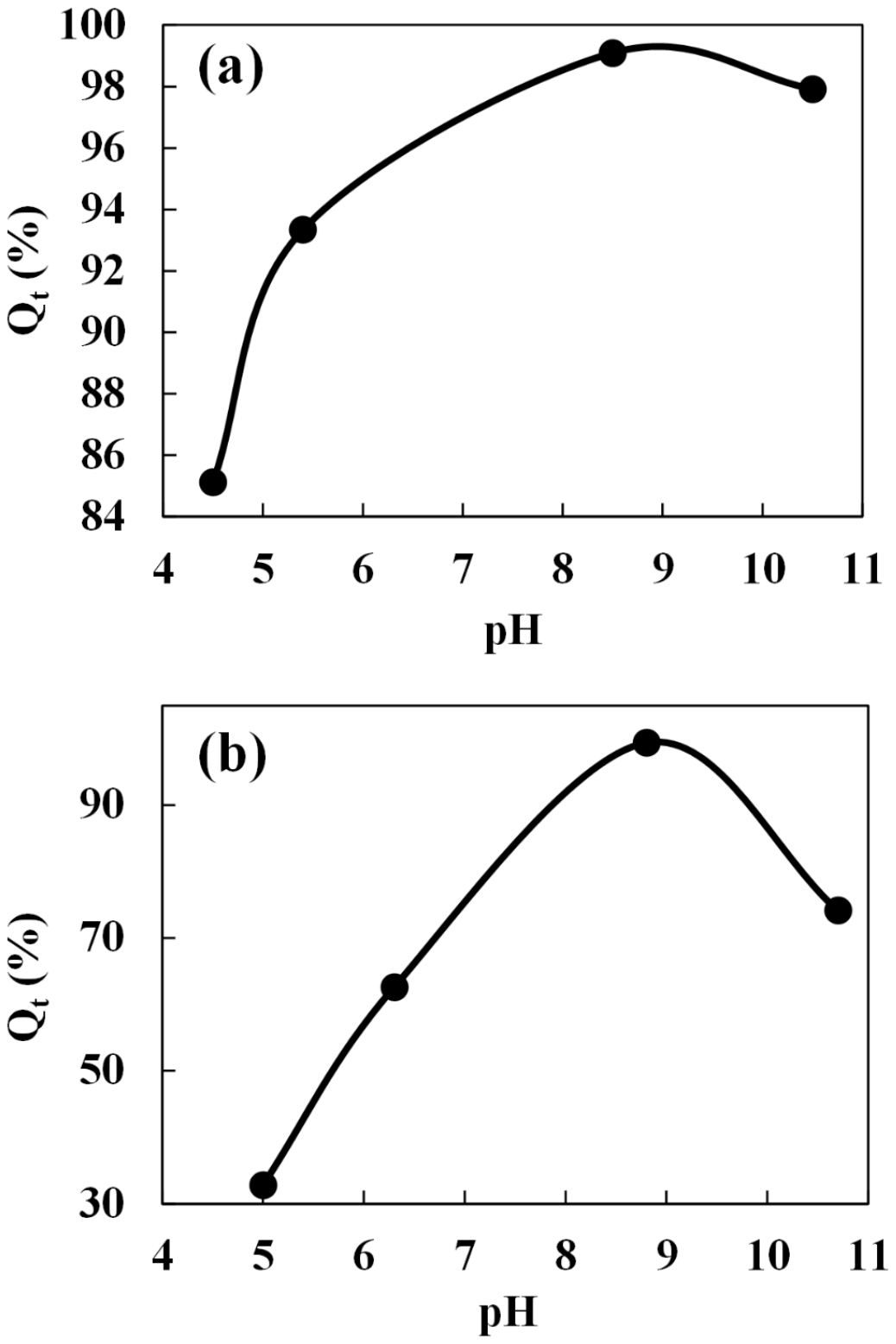

Fig. 25. The effect of pH on the adsorption of (a) As(V) and (b) As(III) by calcined La-LDHs.

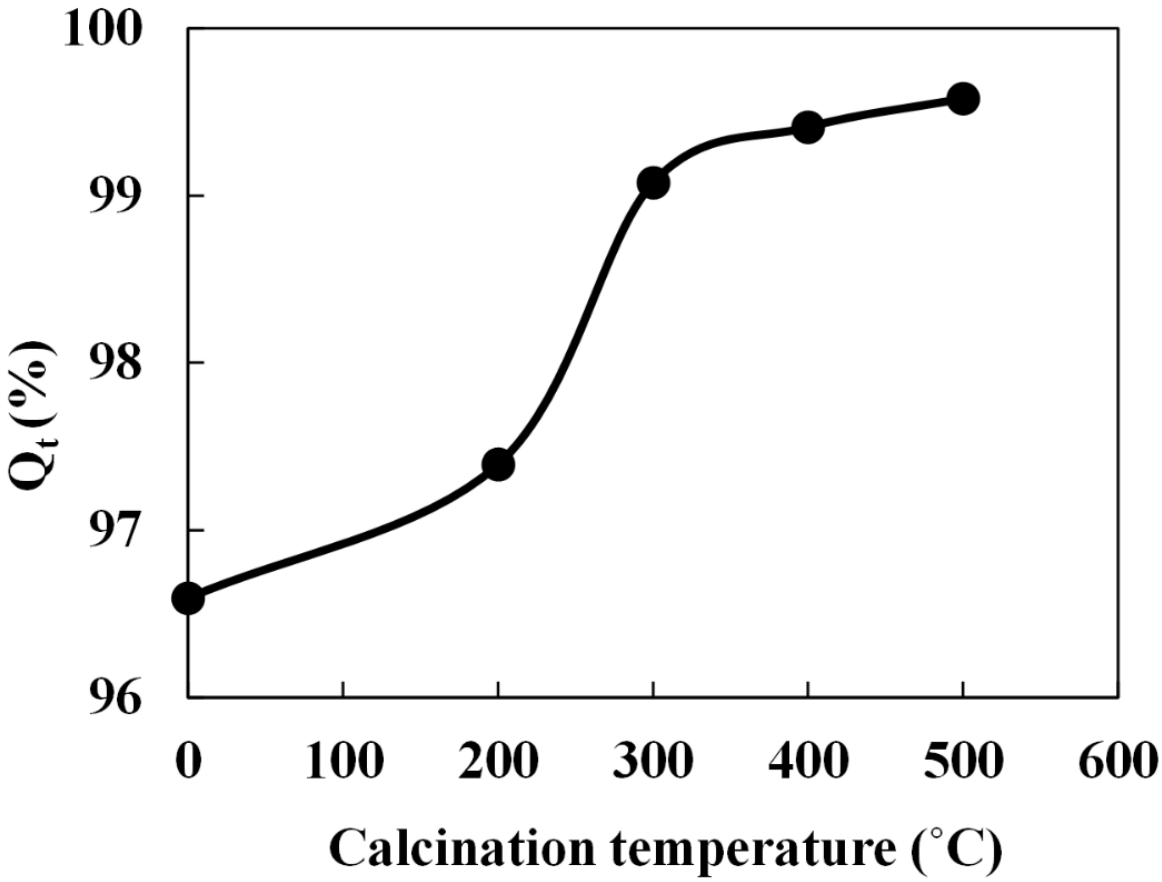

Fig. 26. The effect of calcination temperature on the adsorption of arsenic by calcined La-LDHs

CHAPTER 3

FUTURE WORK

3.1. Scaling Up the Synthesis Process

Since we have obtained promising arsenic removal using the studied LDHs, it is natural to think about scaling up their synthesis process for commercial application. This process should be economically feasible and easily applicable.

3.2. Formulating the Final Product

Again due to the encouraging result and after scaling up the synthesis process, engineering the final product for convenience of application is undergoing. One could think of mixing an adsorbent with a polymer and obtain nanofibers by electrospinning as an example. Also having the final adsorbent in the form of porous agglomerates, disks, or loaded on other materials in the form of disks or sample grains are examples of interesting ways to engineer this promising adsorbent.